Computer Modeling in Engineering & Sciences

Tech Science Press

DOI: 10.32604/cmes.2022.022093

check for updates

REVIEW

Recent Progress of Fabrication, Characterization, and Applications of Anodic Aluminum Oxide (AAO) Membrane: A Review

Saher Manzoor[1], Muhammad Waseem Ashraf[1,*], Shahzadi Tayyaba[2], Muhammad Imran Tariq[3,*] and M. Khalid Hossain[4]

[1]Department of Physics (Electronics), GC University, Lahore, 54000, Pakistan

[2]Department of Computer Engineering, The University of Lahore, Lahore, 54000, Pakistan

[3]Department of Computer Science, Superior University, Lahore, 54000, Pakistan

[4]Atomic Energy Research Establishment, Bangladesh Atomic Energy Commission, Dhaka, 1349, Bangladesh

*Corresponding Authors: Muhammad Waseem Ashraf. Email: dr.waseem@gcu.edu.pk; Muhammad Imran Tariq. Email: imrantariqbutt@yahoo.com

Received: 20 February 2022 Accepted: 07 July 2022

ABSTRACT

The progress of membrane technology with the development of membranes with controlled parameters led to porous membranes. These membranes can be formed using different methods and have numerous applications in science and technology. Anodization of aluminum in this aspect is an electro-synthetic process that changes the surface of the metal through oxidation to deliver an anodic oxide layer. This process results in a self-coordinated, exceptional cluster of round and hollow formed pores with controllable pore widths, periodicity, and thickness. Categorization in barrier type and porous type films, and different methods for the preparation of membranes, have been discussed. After the initial introduction, the paper proceeds with a brief overview of anodizing process. That engages anodic aluminum oxide (AAO) layers to be used as formats in various nanotechnology applications without the necessity for expensive lithographical systems. This review article surveys the current status of the investigation on AAO membranes. A comprehensive analysis is performed on AAO membranes in applications; filtration, sensors, drug delivery, template-assisted growth of various nanostructures. Their multiple usages in nanotechnology have also been discussed to gather nanomaterials and devices or unite them into specific applications, such as nano-electronic gadgets, channel layers, and clinical platforms tissue designing. From this review, the fact that the specified enhancement of properties of AAO can be done by varying geometric parameters of AAO has been highlighted. No review paper focused on a detailed discussion of multiple applications of AAO with prospects and challenges. Also, it is a challenge for the research community to compare results reported in the literature. This paper provides tables for easy comparison of reported applications with membrane parameters. This review paper represents the formation, properties, applications with objective consideration of the prospects and challenges of AAO applications. The prospects may appeal to researchers to promote the development of unique membranes with functionalization and controlled geometric parameters and check the feasibility of the AAO membranes in nanotechnology and devices.

KEYWORDS

AAO membranes; anodization; template assisted growth; filtration; sensors; drug delivery

List of abbreviations

AAO	Anodized Aluminum oxide
EPR	Electron paramagnetic reverberation
PB	Pilling Bedworth
SSAW	Standing surface acoustic waves
PDMS	Polydimethylsiloxane
AT-AAO	Al textured AAO
GZO	Ga-doped ZnO
WG	Wrinkled graphene
SERS	Surface enhanced Raman scattering
SMSA	Simultaneous multi-surfaces anodization
FPI	Fabry-Perot interferometer
GNW	Gold nanowire
TENG	Triboelectric nanogenerator
P3HT	Poly 3-hexylthiophene
ECR-CVD	Electron cyclotron resonance chemical vapor deposition
PPy/DBS	Polypyrrole doped with the dodecylbenzenesulfonate
FITC-BSA	Fluorescein isothiocyanate labelled Bovine serum albumin
PGMA	Propylene glycol monoacetate
DOX	Doxorubicin
PBS	Phosphate buffered solution
PDMS	Polydimethylsiloxane
VACNTs	Vertically aligned carbon nanotube
IAAA	Indole-3-acetic acid
LCD	Liquid crystal display
PAN/GO	Polyacrylonitrile/graphene oxide
ZIF-8	Zeolite imidazolate framework 8

1 Introduction

Since the beginning of the 1940s, membrane technology has advanced as a subdiscipline of physical chemistry and engineering. The development of this technology reached a milestone in the late 40s with the development of microporous membranes. Other landmarks that marched the development of this technology include permionic membranes, asymmetric membranes for reverse osmosis and ultrafiltration, and gas-permeation membranes. Overall, the dyad of research direction and activities for the development of membrane technology can be categorized into two critical stages. The first stage was till the 1980s. Scientists made contributions to the early development of membrane formation using suitable materials. After the 1980s, the second stage is based on membrane formation methods with controlled conditions for improved membrane characteristics [1–5]. Several classification schemes have been reported for membranes due to various material, geometry, and fabrication techniques [6].

Membranes depending upon the features like nature, geometry, and transport mechanism, have numerous medical, and industrial applications like drug delivery [7,8], tissue engineering, dialysis, cold sterilization for pharmaceuticals, water purification, and industrial gas separation [9,10]. Membrane processes have also been proved more valuable than traditional technologies. The reason for the wide range of applications is that the pressure-driven membrane processes provide size-based separation for a wide range from micro to nano [11].

The development process of the nanostructured membrane comprises several challenges and requires the mutual efforts of material scientists and analytical chemists. As for the growth of membrane design and technology, understanding nanostructures, functionalization of nanomaterials, and chemical incorporation play a vital role [10]. Regarding the material of the membrane, the researchers performed an extensive investigation on organic membranes in the beginning. But after some time, inorganic membranes gathered their attention. As inorganic membranes show high resistance to temperature and pressure, have a longer life span, and are insensitive to bacterial attack [12,13].

Aluminum was preferred over other materials in many applications due to its outstanding properties. However, most of the applications require well-defined surface properties that fluctuate by different surface treatments. This paper aims to review the aluminum oxide membrane [14–17], its properties, formation process with controllable geometric features, and detailed applications. Various applications of AAO membranes are discussed in detail with the help of available literature, and with each application, promising prospects are given. Finally, the paper concludes with future directions for the development and applications of AAO membranes in various fields. This study may open new paths for investigations in AAO applications.

2 Overview of AAO Membranes

In the beginning, when anodized aluminum was used in industrial applications, the main focus of the surface finishing industry was to develop a cost-effective anodization process with improved properties of the resulting products. So, the typical approach to getting porous AAO membrane used then did not result in an ordered structure free of cracks. Therefore, that process could not be used for applications in nanotechnology. Hence, attempts were made to develop an Anodization process so that the geometric factors can be engineered. This section provides an overview of anodization processes, characterization and properties of AAO membrane.

2.1 Anodization Process

Aluminum cannot exist in a natural environment in its basic form, and a 1–3 nm thick oxide layer is formed that protects the metal from further reaction with oxygen. Buff [18] in 1857 introduced an electrolytic oxidization process that forms a relatively thick layer than the natural. That enables the use of metal at the industrial level to apply to biomedical degradable devices and sensors [19,20]. In the 1920s, this observed phenomenon of oxidization was exploited for industrial applications [21]. In the 1960s, exposure tests were carried out on AAO in severe atmospheric conditions. The process is called anodization, as the electrolytic bath has aluminum as an anode. In the electrolysis process, the Al is soaked into an acid electrolyte bath. Electric current is passed through the bath in the presence of a cathode, as shown in Fig. 1. The whole reaction can be expressed using the following equation (Eq. (1)):

$$2Al + 3H_2SO_4 \rightarrow Al_2(SO_4)_3 + 3H_2 \quad (1)$$

Anodization of metals and semiconductors like Al, Ta, Nb, Mg, W, Hf, Zr, Si, Hf, and InP has been reported to form nanoporous structures. The oxidization process produces two types of films depending upon electrolyte and anodizing conditions. These films are known as porous type and barrier type. In the barrier type, the AAO membrane oxide layer is formed at the top of the Al substrate. The thickness of these films increases with the current density applied; however, anodizing time does not affect the thickness between the outer and inner layers. Minimum loss of ions occurs in the electrolyte from the film while forming barrier-type films. Addition of oxygen and loss of electrons

or hydrogen ions. The formation of porous type AAO is a complex process. Porous thick films are formed when the anodic film is chemically reactive to the electrolyte like phosphoric, sulphuric, or oxalic acid. These films have a barrier layer in contact with the metal and a thick porous layer above it. The thickness of the porous layer is directly proportional to the amount of anodizing time [18,20,22]. The schematic for barrier and porous type AAO is shown in Fig. 2 and the properties of barrier and porous oxide films are given in Table 1 [23–27].

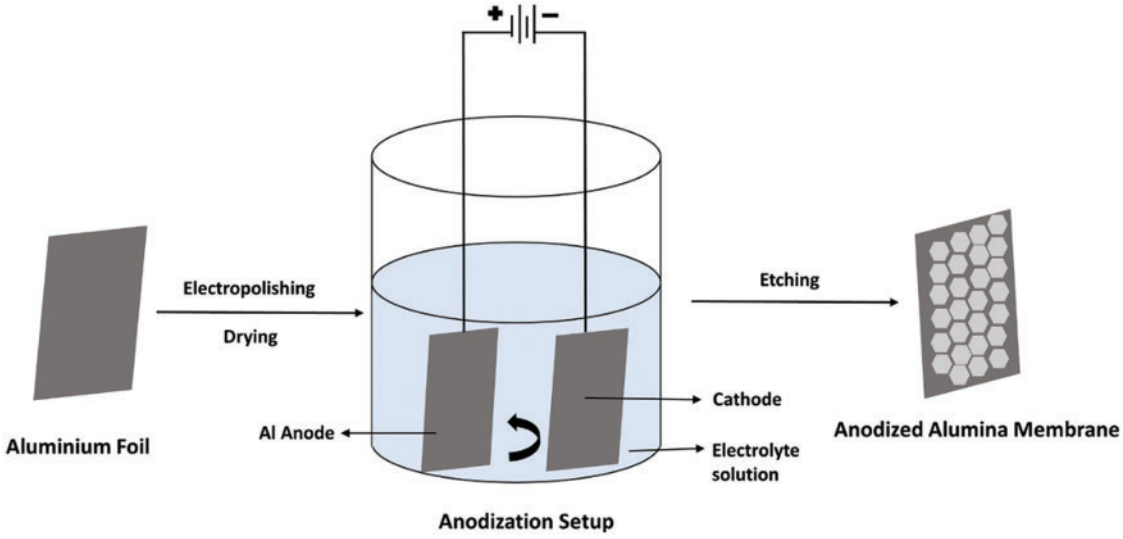

Figure 1: Schematic of the anodization process

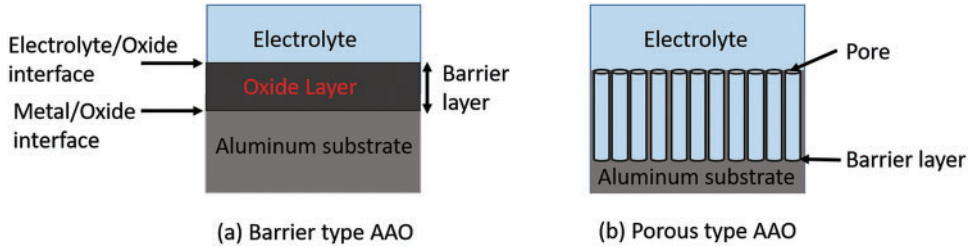

Figure 2: Schematic representation of barrier type and porous type AAO

Table 1: Properties of barrier and porous oxide films [13,28–32]

Filmtype	Common electrolytes	Morphology	Pores growth	Membrane structure	pH	Applications
Barrier	Phosphate, Tartrate, Ammonium Borate	Amorphous Uniform in thickness Sharply defined	Exponential	Circular	>7	Capacitors Rectifiers

(Continued)

Table 1 (continued)

Filmtype	Common electrolytes	Morphology	Pores growth	Membrane structure	pH	Applications
Porous	Sulphuric acid, Oxalic acid, Phosphoric acid	Duplex	Linear w.r.t voltage	Hexagonal cells with cylindrical nanopores	<5	Paints Lacquers Adhesives

Both types of layer structures have applications in industry. Barrier type helps make capacitors because of its thin, resistant yet hard layer that behaves as an insulator. On the contrary, porous films are thick and have a highly controllable density distribution, pore diameter, cylindrical shape, and periodicity. Because of their high aspect ratio and porous structure, these templates are widely used in nanotechnology [23–27].

Pore development behavior under various precise conditions has been studied to plan an interesting permeable stage for explicit applications significantly. All the different types of anodization used to get porous AAO structure are explained briefly.

(a) Hard anodization: The typical hard anodization process adopted by the industries in the early 1920 was carried out at a potential more incredible than the breakdown value resulting in cracks in the resulting anodic structure with poor mechanical stability. Various attempts were made to overcome the problem associated with the process. The modified hard anodization process is carried out at a high voltage, but the voltage value is below the dissolution of the metal. The primary benefit of this type of anodization is that we can get a high-quality nanoporous oxide structure with a fast growth rate [33,34]. A perfectly ordered AAO membrane with a high aspect ratio with an increased oxide growth rate by 70 mm/h was obtained by a hard anodization process [35].

(b) Mild anodization: Mild anodization is carried out at relatively low voltage, and thus the oxide growth is slow. In 1996, Masuda et al. developed a two-step anodization process in which the anodization is carried out in two steps. Two-step anodization combines mild and hard anodization steps with varied voltage or time in each step. In between these steps, etching is done to remove the distorted portion. The conditions during both steps for anodization are the same except for each step's time interval. The development of this method led to several other studies by researchers for a better understanding of parameters and their dependence on the anodization conditions [36,37].

(c) Pulse anodization: In the pulsed anodization process, low and high potentials are applied in pulses for both hard and mild anodization conditions. Many researchers were combining both hard and mild anodization processes to achieve desired membrane properties. In 1987, Tu et al. [38] reported pulsed AC and DC anodization; however, the results showed that the structure had satisfactory corrosion resistance with cracks and high surface roughness. Lee et al. [39] also used pulses of hard anodization voltage and mild anodization voltage in the presence of sulphuric acid as an electrolyte at room temperature to achieve AAO membrane.

(d) Cyclic anodization: Potentiostatic or galvanostatic periodic oscillatory signal is applied in this type of anodization process. A slow change of voltage/current between the mild and hard anodization modes is applied using the periodic signal, resulting in the porous structure. Losic et al. [40,41] applied this type of anodization process for the formation of AAO membrane. Although the concept of cyclic

anodization is not new, it has also been used previously for the anodization of sputter-deposited alloys. The parameters chosen for the cyclic anodization result in the variation of the morphology of the anodized membrane. The variation of potential during pulse and cyclic anodization is shown in Fig. 3.

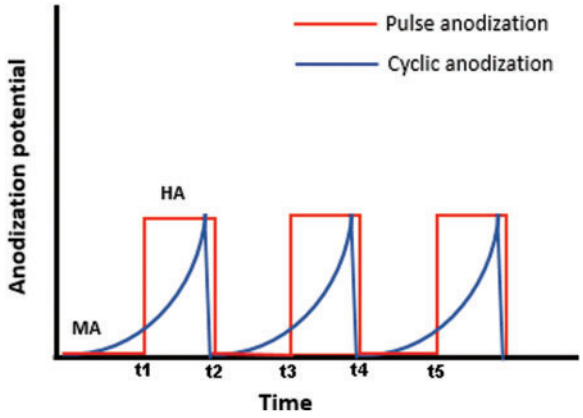

Figure 3: Variation of anodization potential with time in pulse and cycle anodization

When voltage is applied, the pore initiation occurs and with increase of voltage more pores initiate on the substrate and the pore diameter increases resulting in pear drop shape at high voltage. Metal dissolution varies for different voltage types pore growth during different types of anodization process in given in Fig. 4. In hard anodization high voltage is applied so the pores are comparatively thin from the top where as in mild anodization the upper portion of pores is quite wide. In cyclic and pulse anodization MA and HA process are applied alternatively so the pore length varies accordingly.

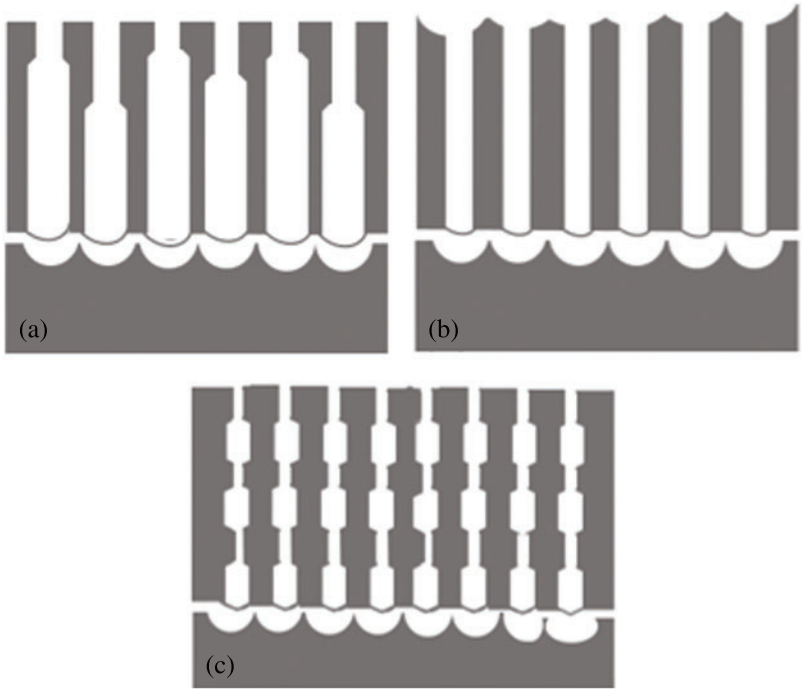

Figure 4: Pore growth (a) Hard anodization, (b) Mild anodization, (c) Pulse/cyclic anodization

2.2 Characterization of AAO

The anodization process results in a nanostructure that consists of a periodically arranged hexagonal pore channel. Nucleation of pores occurs on the substrate and grows in the vertical direction maintaining their direction coherent. The geometric feature of the prepared structure strongly depends on the experimental conditions. Distinct quantities for the characterization of the AAO membrane are pore diameter, pore density, porosity, pore length, and interpore distance. Fig. 5 shows the horizontal view of the AAO membrane with hexagonal cells with pores in their centers, and each hexagonal cell is separated by a cell boundary. Fig. 6 represents the 3D dimensional view of the AAO membrane with well-defined oxidized hexagonal cells on an Aluminum substrate.

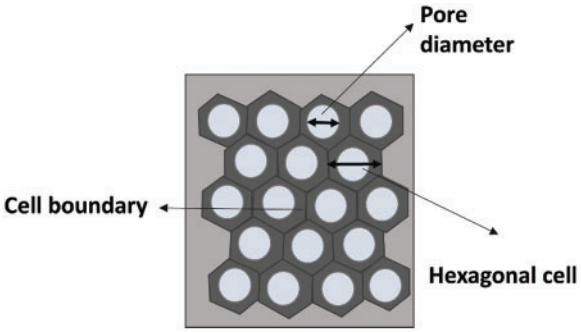

Figure 5: Horizontal view of ideal AAO membrane

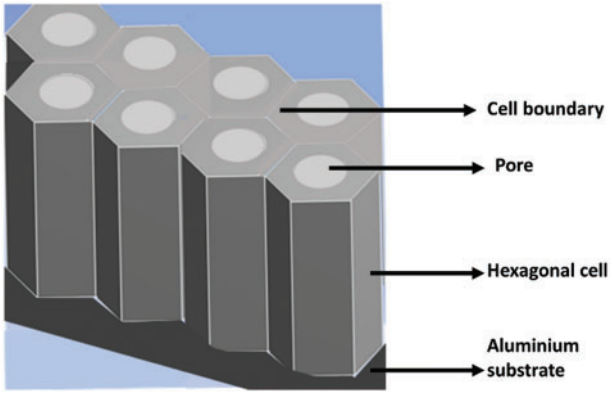

Figure 6: 3-dimensional view of AAO

The parameters of the membrane depend on the anodization conditions. The most critical parameters for the characterization of the anodized membrane, i.e., pore diameter, interpore density, porosity, and pore density. Fig. 7 represents the bargraph for obtained pores size for different anodization conditions reported in literature. Table 2 shows the AAO membrane fabricated using different anodization types and the resulting parameters of the membrane [15,33,36–38,41–53].

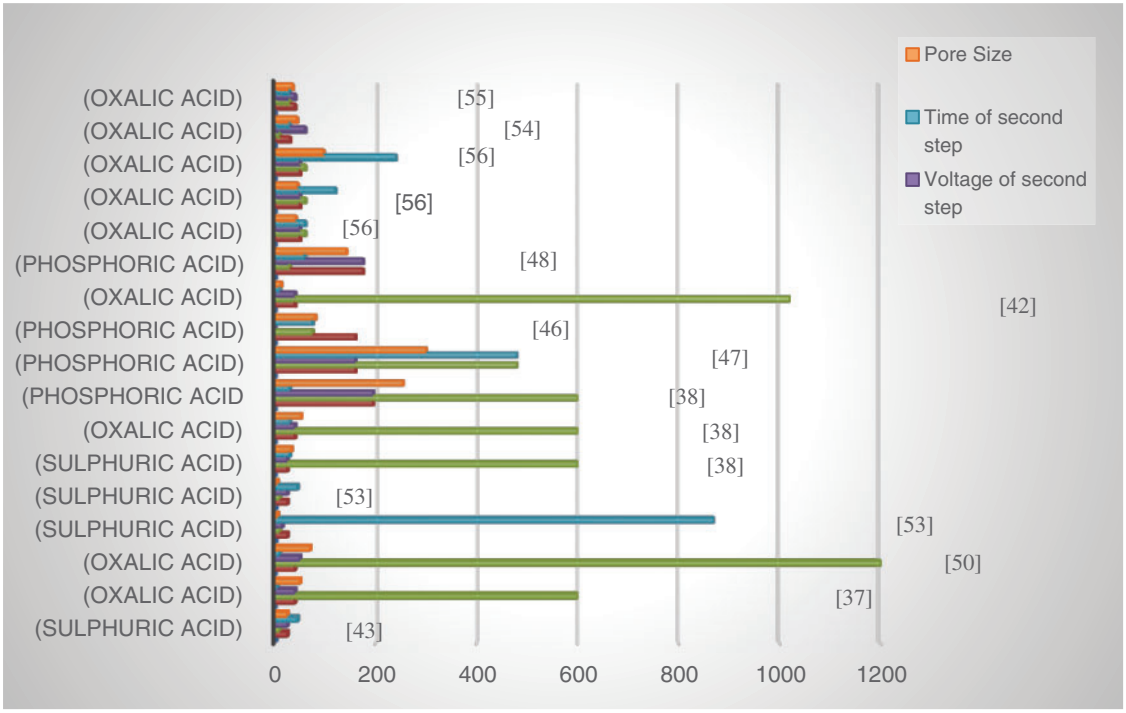

Figure 7: Effect of two step anodization parameters on pore size of the membrane [37,38,42,43,46–48,50,53–56]

Table 2: Effect of anodization type and three mostly used acidic electrolytes on characterization parameters

Electrolyte used	Anodization type	Temperature (°C)	Voltage (V)	Pore size (nm)	Interpore distance (nm)	Substrate thickness (μm)	Refs.
Oxalic acid	Hard anodization	1	100–150	49–59	200–300	110	[33]
	Hard anodization	–	130	40	>400	500	[36]
	Hard anodization	0–5	140–180 and 140–200	~100	–	Disk of diameter 20000	[42]
	Two-step anodization	17	40	50	100	–	[37]
	Two-step anodization	5–7	40 and 20–50	~70	–	500	[43]
	Cyclic Anodization	<0.5	20–50	Branched pores	–	5	[44]

(Continued)

Table 2 (continued)

Electrolyte used	Anodization type	Temperature (°C)	Voltage (V)	Pore size (nm)	Interpore distance (nm)	Substrate thickness (μm)	Refs.
	Pulse and pulse reverse anodization	18–25	−7 to 30	30–60	–	250	[45]
	Two-step anodization	17	40	52	100	400	[38]
	Two-step anodization	3	40	24	105	–	[15]
Sulphuric acid	Two-step anodization	1	15–25	18–26	49–65	250	[46]
	Pulse anodization	1	25–35	16–35	–	–	[47]
	Hard anodization	1	27–80	15–30	70–145	–	[48]
	Two-step anodization	−8 1 10	15–25	14–11.5 5.7–4.9 13–15.3	35–37 3.7–2.7 35.7–34.6	250	[53]
	Two-step anodization	0.85	25	33	63	400	[38]
Phosphoric acid	Cyclic anodization	−1	20–300	300–1200	–	5	[41]
	Two-step anodization	0	100–160	85–140	–	–	[49]
	Step Anodization	25	160–20	160–30	580–87	–	[50]
	Two-step anodization	12	195	254	490	400	[38]
	Two-step anodization	−5 and 0	100–160	>100	250–490	–	[51]
	Two-step anodization	0	160–195	140–190	405	–	[52]

2.3 Properties of AAO Membranes

These membranes are highly flexible nanomaterials that consolidate the artificially steady and precisely vigorous properties of ceramics with a homogeneous nanoscale association that can be tuned in terms of pore distance and lengths. The AAO membranes have a high surface area that can accommodate atoms of diverse sizes. AAO membranes exhibit extraordinary properties with tunability which make them suitable for countless applications. The properties responsible for great attention received by AAO membranes to get the maximum benefit from AAO membranes are discussed below.

(a) Electrostatic properties: Electrostatic properties of the inward pore surface just as the neighborhood causticity inside the nanochannels can be tuned. Due to the amorphous nature of the alumina layer, the nanochannel surface of AAO membranes prepared by anodization shows a positive charge. The anodization conditions greatly influence the surface electrostatic properties of the AAO membrane, and the acidity of the aqueous medium inside the pore channels depends on the pore diameter. Tunability of surface charge and associated electrostatic potentials make the membrane beneficial for specific applications that rely on acid-base equilibrium [57].

(b) Wettability: The wettability of any droplet deposited on a solid surface depends on the energy difference of both liquid and the surface. In the case of the AAO membrane, energy difference governs whether the liquid will enter the nanopores or not. The diameter of the nanopore if increases, then ultimately, the contact angle of the water with the surface increases [58]. Electrochemical anodization of the aluminum substrate can result in superhydrophobic AAO membranes if modified with fluorinated silane solution. The hydrophobic membrane shows long-term stability and can be used in anti-corrosion membrane applications. The contact angle of $\sim$165 and sliding angle $<$2 have been reported for membranes modified by fluorinated saline [59]. Also, hydrophilic AAO nanoporous membranes can be prepared using the anodization method. By varying the anodization and the post-processing conditions, AAO membranes with different wettability and contact angles for water can be prepared depending on the application for which it is to be used [60,61].

(c) Mechanical properties: The nanoindentation method is used to investigate the mechanical properties like surface hardness, scratch hardness, and surface roughness of the AAO membrane. The hardness of the membrane depends on the pore diameter; as the pore diameter increases, the hardness decreases. Heat treatment after membrane formation influences the mechanical properties of the membrane, hardness increases as a result of heat treatment. Also, the wettability of the membrane depends on the surface roughness, and smooth surfaces produce low surface energy [62,63]. Relatively thin AAO membranes with increased mechanical strength have also been reported by using Si support. Which results in better performance of membranes in biomedical applications [64].

(d) Biocompatibility: AAO nanopores display excellent biocompatibility towards cells of the four basic tissue types (neuronal, epithelial, muscle, and connective tissue) as well as with platelets and different microorganisms. AAO interfacial examinations, a tremendous scope of biomedical applications have arisen. Nonporous AAO membranes have just been joined into coculture substrates for tissue designing, alumina biosensors, what's more, bone embed coatings or nanoporous bio capsules for drug conveyance. Some portion of these applications has likewise been concentrated in vivo in brief timeframe tests yielding promising results concerning biocompatibility, drug discharge properties, what's more, mechanical security of the nanoporous AAO films [65]. Biocompatibility of AAO films with a mean pore measurement of 100 nm was studied. A natural assessment of the layers was finalized to decide cell grip and morphology utilizing the Cercopithecus aethiops kidney epithelial cell line. Examination's positive results show that AAO films can be utilized as a feasible tissue platform for potential tissue designing applications later on [66].

3 AAO Membrane Applications

AAO is an electro-synthetic process that changes the surface of the metal through oxidation to deliver an anodic oxide layer. During this process, a self-coordinated, exceptionally demanded cluster of round and hollow formed pores can be made with controllable pore widths, periodicity, and thickness. These properties engage AAO layers to be used as formats in various nanotechnology applications without the necessity for expensive lithographical systems. The current status of the

investigation on AAO for various nanotechnology application make them beneficial in the assembly of nanomaterials and devices or unite them into unequivocal applications [25,67]. In this paper most prominent applications of AAO membranes in biomedicine; sensing, separation, drug delivery and nanostructures formation have been discussed. Properties of AAO membranes with various reported applications in different fields of interest are given.

3.1 AAO Membrane for Template-Assisted Growth of Nanostructures

3.1.1 Applications of AAO Membrane for Template-Assisted Growth of Nanostructures

Template-assisted growth represents a straightforward method in which the template acts as a structural framework. The nanostructures of the desired material can be formed within the template from precursors *in situ,* with shape and size defined by the pore size of the template. Generally, templates are of two types; soft templates and hard templates. Naturally occurring micelles are referred to as soft templates, whereas templates related to materials like AAO membranes are considered hard templates [68]. Due to size, the influence of diminishment nanostructures has a higher active part and increased surface to volume ratio, in addition, low-cost synthesis, monodispersed, and controllable diameter of AAO nanoporous membranes makes them suitable for the template-assisted growth of different nanostructures. Nanostructures ranging from nanotubes, nanowires, nanorods, nano dots arrays, interconnected 3D nano networks with highly controllable size and shape of a certain material can be grown using such membranes [69,70] Successive deposition of specified material into the nanosized pores of the AAO membrane results in nanostructures embedded in the membrane. However, free nanostructures can also be obtained by removing the membrane acting as a template [71,72].

AAO template-based fabrication of nanowires arrays of pure metals like Pb [73], Sb [74], Ni [75,76], Zn [76], Ag [76] has been reported using electrodeposition. Thongmee et al. [77] also used electrodeposition to fabricate metallic nanowires of Ni, Co, Cu, and Fe. Yang et al. [78] reported low ion concentration and heating rate are beneficial for the AAO template-based fabrication of Ag nanowires using calcination. For the first time, Wu et al. [79] used AC-DC electrodeposition for the deposition of Au nanowires into an AAO template. Besides, the galvanic displacement method has been employed by Ganapathi et al. [80] to synthesize Cu nanowires into AAO. Electrodeposition method has also been employed for the fabrication of Ag dendrites to be used as 3D Surface Enhanced Raman Spectroscopy (SERS) active substrates for the detection of trace organic pollutants [81]. Fig. 8 depicts step-wise fabrication of Au nanoparticles on AAO template. Due to the uniform geometry of the AAO membrane, precisely controlled particle size can be obtained that is required for fine-tuning of plasmonic absorption peak. The Au nanoparticles transferred to epoxy support are completely stable in a fluidic environment. The presented mushrooms arrangement of AuNps on epoxy pillars with reproducible sensitivity successfully demonstrated label-free DNA detection. Other nanostructures of different materials reported in literature formed using AAO template along with their applications are given in Table 3 [77–80,82–98].

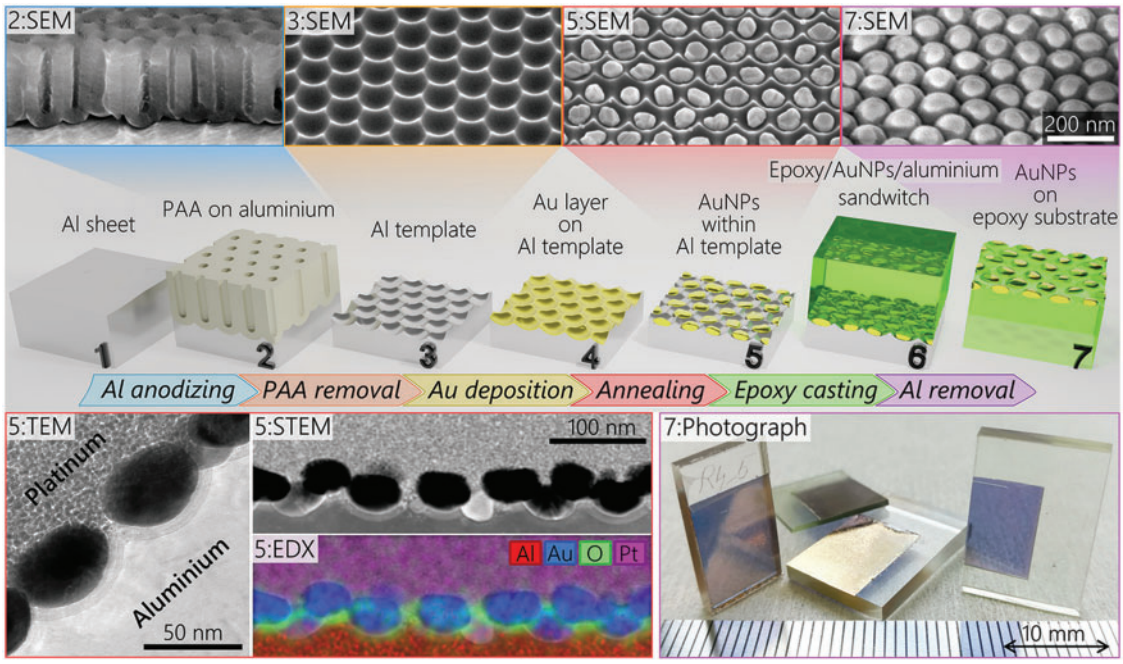

Figure 8: AAO based fabrication of AuNps on epoxy substrate for label-Free Plasmonic DNA Biosensors. Step wise schematic illustration of fabrication process (top), SEM figures of membrane at different steps (center), TEM STEM and EDS of AuNps within Al template (bottom left), photograph of sample after 7 steps (bottom right). Reproduced from [98]. Copyright 2020 American Chemical Society

Table 3: AAO membranes for template assisted growth of various nanostructures

Pore size of AAO (nm)	Method	Nanostructure formed	Diameter of nanostructure (nm)	Application	Refs.
100	Calcination	Ag nanowires	35.1	Potential application as a catalyst	[78]
50	Electrodeposition	Cu nanowires	50	Single crystalline nanowire formation with good magnetic properties	[77]
30	AC-DC electrodeposition	Au nanowires	30	–	[79]
67 110	RF magnetron Sputtering	Au nanoparticles	55 92	Label free plasmonic DNA biosensos	[98]

(Continued)

Table 3 (continued)

Pore size of AAO (nm)	Method	Nanostructure formed	Diameter of nanostructure (nm)	Application	Refs.
80	Electropolymerization	Poly(3-hexylthiophene) (P3HT) nanorods and nanotubes	100	Effect of monomer concentration on nanostructure and corresponding band gap	[82]
50	Pulsed laser deposition	$CoFe_2O_4$ nanodots	45	Potential in oxide nanomagnets and spintronics	[83]
60	Microwave plasma electron cyclotron resonance chemical vapor deposition (ECR-CVD)	Carbon nanotubes	75	potential applications for cold-cathode flat panel displays	[84]
75	E-beam evaporation	ZnO nanodots on Si(100)	9.7	–	[85]
78	Galvanic Displacement process	Cu nanowires	73	Electrochemical denitrification	[80]
80	Infiltration and sulfurization	$CuInS_2$ nanorods	80	Potential for fabrication of Photocathodes	[86]
200	CVD	Carbon nanocoils	100–500	–	[87]
80	Hydrothermal process in aqueous solution	ZnO nanowires	80	Field Emission Applications	[88]
300	Plasma assisted reactive evaporation	Tree like structures of InN nanoparticles	Thickness 500	–	[89]
30	Electrochemical deposition	ZnO nanorods	60	Fast Response Photodetector	[90]
230–370 40–100	Sol gel routes	γ-$Na_{0.7}$ CoO_2 nanotubules	200–340 35–97	Thermoelectric applications	[91]
60–70	Electrodeposition	Co nanowires	70	Catalyst for methane combustion	[92]
90	Ultrasonic hydrothermal method	Fe_3O_4 nanoparticles	30–40	Arsenic removal	[93]
100	Electrodeposition	Cu nanowires	100	Antibacterial activity	[94]
60	Etching	Aluminium oxide nanowires	67	Microelectronic devices	[95]

(Continued)

Table 3 (continued)

Pore size of AAO (nm)	Method	Nanostructure formed	Diameter of nanostructure (nm)	Application	Refs.
240	Electrodeposition	ZnO nanowires	300	Scintillator	[96]
75	Autoclave enclosed hydrothermal growth	Zr-$BiFeO_3$ nanoflakes	25–100	Energy storage application	[97]
51	Solid state dewetting	Au nanoparticles	51	Plasmonic DNA bosensors	[98]

3.1.2 Prospects of AAO Membrane for Template-Assisted Growth of Nanostructures

AAO membranes have excellent prospects as a template for the growth of large-scale nanostructure arrays for practical applications. The template-assisted growth of nanostructure is a widely accepted theoretical concept, but studies are required for the subset of materials to develop various structures. Optimization of template synthesis is crucial for the growth of multidimensional structures on a large scale. The control over crystallinity, diameter, and functionalization of nanostructures fabricated using AAO templates may open new paths for the expansion of their applications in various fields.

3.2 AAO Membrane for Filtration

3.2.1 Applications of AAO Membrane for Filtration

Pressure driven membrane filtration process depends upon the pore diameter of the membrane and is divided into four types. The factor for good selectivity is that the membrane must have narrow pore distribution. The thickness of the membrane should be between 1 to 10 μm for high flux. The size-based separation using membrane is used in many industrial and medical applications. The membranes with a mean pore diameter of 1 μm are used in the filtration process called microfiltration. Ultrafiltration is performed using a membrane with a mean pore diameter of 100 nm. For nanofiltration, the membrane should have a pore diameter of 10 nm, and the membranes with 1 nm mean pores are used in the process called reverse osmosis.

Biofiltration can be categorized into two main mechanisms based on the size and chemical affiliation of filtration membranes. Size limitation results in the blockage of molecules whose size is greater than the membrane's pores. Chemical affiliation is related to the filtration mechanism as in the bonding of molecules with the filter membrane, and the selected molecules can be separated based on lower or higher chemical affinity with the membranes. If these factors can be controlled, then the filtration process can be optimized easily [99–102]. The simplest membrane filtration system comprises a filtration membrane set up in the system, fluid to be filtered is poured onto the membrane, and the filtrate is obtained.

The separation of desired molecules has applications in the biomedical field. Important factors for filtration application of AAO membrane include flux rate, selectivity, high chemical, and mechanical stability with uniform pore size. The porosity of the sheet and membrane thickness is used to determine the flow rate and produce a mechanically stable AAO membrane for biomedical applications. Theoretical studies have been done for testing the mechanical stability of AAO membranes for

filtration application. The studies show that the membrane can bear pressure up to 0.79 MPa and is suitable for microdialysis [103]. An adaptive ultrafiltration layer has been designed using an AAO template in polyprotic to provide filtration properties and used for desoxyribonucleic acid analysis [104]. Two-layered AAO has also been reported to speed up the hemodialysis and hemofiltration process [105]. Two-layered AAO membrane structures have been used for effective dialysis and to sieve exosomes, potential biomarkers for the early detection of cancerous cells [106]. Functionalized AAO membranes for purification of contaminated water and enantioselective separation have also been reported in the literature [107,108]. Figs. 9 and 10 represent the mechanism of filtration using functionalized AAO membranes for filtration and separation respectively. Fig. 9 represents a three-layered composite membrane for efficient water purification. AAO membrane with the middle layer of AuNps and the top layer of TiO_2 Nps shows the photocatalytic function and photothermal driven evaporation. TiO_2Nps exhibit photocatalytic function, and Au Nps enables plasmonic evaporation using solar energy. The plasmonic Au film heats up due to solar irradiation resulting in a hot zone at the interface of water and air. The heating up of the interface results in efficient water evaporation. The bifunctional integration results in an expanded useful solar light range for generating pure water in one step [107]. Two optically active homochiral polyfluorenes coated on AAO membranes are shown in Fig. 10. The cylindrical channels of AAO membranes help confine the polymers, which increases the available chiral surface, resulting in increased enantioselective separation of the amino acid mixture. One enantiomer was absorbed within the chiral pores, and the other enantiomer was left in the filtrate. This study revealed that the modulation of polymer-coated membrane and pore size can effectively enhance the separation process [108]. Various other applications of AAO membranes for filtration purposes have been reported in the literature and are also given in Table 4 [99,102,105,106,109–121].

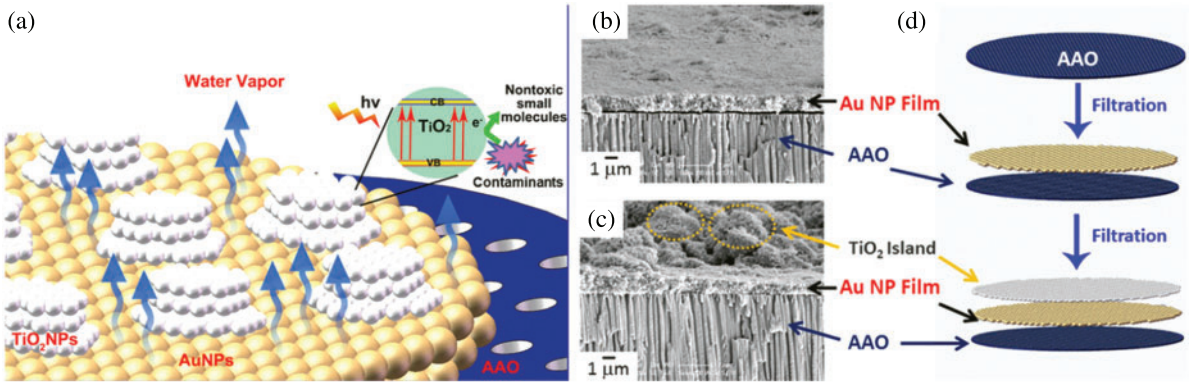

Figure 9: Biofunctional membrane for purification of contaminated water. (a) Design of Bifunctional TiO_2-Au-AAO membrane with AAO at bottom Au in the middle and TiO_2 at top, (b) Cross sectional SEM image of two layered structure (Au Np/AAO), (c) Cross sectional SEM image of three layered structure (TiO_2/AuNp/AAO), (d) Schematic illustration of preparation method. Reproduced from [107]. Copyright 2015 American Chemical Society

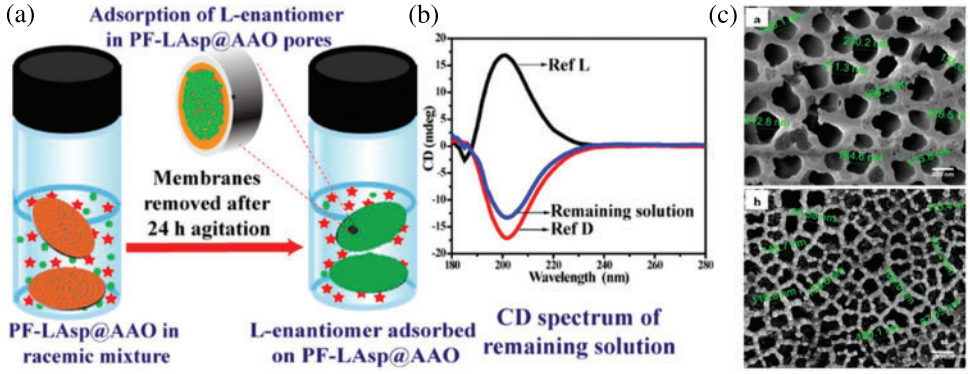

Figure 10: Functionalized AAO membrane for enantioselective separation. (a) Illustration of enantiomer separation process using Chiral Amino Acid Functionalized Polyfluorene Coated AAO (PF-Lasp@AAO), (b) CD spectrum of remaining solution after separation process, (c) FE-SEM micrographs of AAO membrane and polymerized AAO membrane. Reproduced from [105]. Copyright 2020 American Chemical Society

Table 4: Different types of AAO membranes for filtration

Membrane type	Pore size of AAO membrane (nm)	Application	Refs.
AAO based 3D microchannels	50	Microchannels for molecular separation	[109]
Two nano-porous AAO membranes sandwiched in between PDMS layers	30 80	Two AAO membranes sandwiched between PDMS for Exosomes Isolation	[106]
AAO membrane in micro hydraulic mechanical system	50	Vibro-active nano filter for filtration, separation, and transportation of particles, using standing surface acoustic waves (SSAW)	[110]
Optical gas sensing package covered with AAO membrane	40	Filtration interface to let air and other gases pass and prevent contaminations in forms of particles for an optical gas sensor	[111]
AAO tubular membrane	20	Potential application for hemodialysis	[112]
AAO membrane and polydimethylsiloxane (PDMS) microwells with through holes	25	Microwell-assisted filtration of algal solution	[113]

(Continued)

Table 4 (continued)

Membrane type	Pore size of AAO membrane (nm)	Application	Refs.
Nafion-coated AAO filter	20	Nafion-coated AAO filter for ion separation in presence of electric field	[114]
Microfluidic channels of AAO with immobilized probe DNA sequences	200	Filtration membrane to form probe DNA electrode for electrochemical sensing	[115]
Polyrhodanine modified AAO	150	Heavy metal ions removal with potential applications for removing the hazardous heavy metal ions from wastewater	[116]
Al textured AAO (AT-AAO) membrane	31.25	Fluid flow and permeability of acetone, methanol, dimethylformamide, water, cyclohexane, ethanol, isopropyl alcohol, and n-butanol	[117]
Polyrhodanine modified AAO with activated carbon deposition	55–70	Multi-filtration membranes with potential applications in removing heavy metal ions from water, soil, food and drug	[118]
Two layered AAO membrane structure	50 350	Wearable hemodialysis device	[105]
AAO membrane integrated with an on-chip microfluidic platform	38.2	Electrokinetic separation of biomolecules and potential for binary separation and detection of a molecular reaction as a result of specific recognition	[119]
Functionalized nanoparticles embedded AAO	100	As working template for enhanced filtration	[120]
Silica–surfactant nanocomposite in the AAO membrane	3.5	Size-based molecule separation	[102]
Functionalized chitosan AAO membranes	200	Purification of Hemoglobin from red cell lysate	[99]
Tubular AAO films	60	Liquid or gas filters, drug delivery, and energy applications	[121]

3.2.2 Prospects of AAO Membrane for Filtration

The AAO membranes have promising prospects in gases and liquids filtration applications. Chemical affinity is an essential factor, and functionalization of AAO membrane with various nanostructures are important factors to be studied for enhanced and optimized filtration. Research

on the bonding of multiple molecules with the membrane and the decoration of nanostructures within pores can lead to efficient and highly selective filtration. The improved filtration performance may be proved highly promising to be applied in future areas.

3.3 AAO Membrane in Sensors

3.3.1 Applications of AAO Membrane in Sensors

Due to its unique properties, extensive studies have been performed on AAO to develop low-cost sensing devices. The characteristic responses of AAO membranes while interacting with light make them suitable for optically active devices. Effectively immobilized sensing elements within the pores can optimally interact with the analytes flowing through the pores due to the large surface-to-volume ratio of the nanopores. Also, AAO with nanoporous structure has the potential in single-molecule sensitivity. These properties make them suitable for the development of electrochemical and biosensors. Nanopores of AAO membranes are suitable for molecular transport and attachment, resulting in one device integrated with both separation and sensing functions. Additionally, AAO membranes have also been effectively used as a substrate to fabricate various humidity and gas sensors [122]. Highlights of sensing and biosensing applications of AAO membranes present in the literature are given.

Gorokh et al. [123] prepared two distinct aluminum oxide films using tartaric and malonic acid. The anodic films were first prepared, then tungsten oxide was sputter deposited on the films to form metal oxide test sensors. The results indicated that the sensitivity of the sensors using tartaric acid increases with the increased porosity of the membrane. Both the test sensors were unresponsive for carbon monoxide but showed an enhanced response for ammonia. Hang et al. [124] deposited metal oxide gas sensing film of Ga-doped ZnO (GZO), and GZO annealed in H_2 (GZO-H) via electrophoretic deposition on AAO/Al structure. In the presence of an aqueous solution, the substrate and deposited film were destroyed because of the H_2. On the contrary, the deposition was successful in the presence of ethanol as a dispersant. In gas sensing AAO layer act as an insulator, so its thickness plays a vital role in enhancing its resistance. Formaldehyde was used as a probe to verify the gas sensing property of the as-prepared structure. It was concluded that AAO/Al structure could be used to fabricate metal oxide gas sensors successfully. Lo et al. [125] used anodic aluminum oxide with nanopores of about 50–60 nm to implement inductive proximity sensors. The anodic aluminum oxide was used as a template for patterning spiral film of gold. Due to nanotexture, the gold film has significantly enhanced surface area that improved the inductance of the proximity sensor. Hong et al. [126] developed a metal-insulator-metal device in which the nanoporous AAO fabricated on the Si substrate act as an insulator. Au-AAO-Al layers on the Si substrate were implemented. The top metal layer deposited on the AAO has nanotexture, due to which the capacitive touch sensor has improved sensitivity. AAO based humidity capacitive sensors were investigated by Balde et al. [127] Paper was used as a substrate to fabricate the AAO layer. The results showed clearly that the geometry of AAO and the sensitivity of the sensors varies by voltage variation. The capacitive response of the sensor increased with temperature up to 45°C but decreased for measurements after two weeks. Also, the low sensitivity of AAO based capacitive humidity sensors under low humidity conditions has been addressed by Park et al. [128]. The AAO barrier oxide layer stored humidity within the pore and resulted in linear capacitance variation at relatively low humidity

Kumeria et al. [129] integrated AAO substrates coated with ultrathin gold layer into microfluidic devices. Two different strategies were used in this work to explore sensing properties based on reflective interferometric spectroscopy. Gold-modified AAO with Thiol binding and antibody-modified AAO with circulating tumor cells binding were studied. Results showed potential for biosensing devices

with the admirable capability of detecting different analytes. Besides, Shaban et al. [69] fabricated nanoporous CdS/AOA bi-layer film using AAO as a template for spin coating of CdS film. Due to the positive experimental results, the bi-layer film was attributed as an efficient, low-cost, and relatively simple glucose biosensor. Label-free DNA detection is the most challenging application of Localized surface plasmon resonance sensors due to the petite size of the DNA molecules. Lednicky et al. [98] fabricated gold nanoparticles-epoxy surface nanocomposites using AAO as a template. The fabricated LSPR sensors were accurate in the detection of 20 bases long label-free DNA. Ma et al. [111] fabricated optical gas sensor with an AAO membrane as the air filter. The fabricated system could prevent contamination with particles above the size of 70 nm. However, the sensor's sensitivity could be improved by tuning the pore size of the AAO membrane. Schematic representation for fabrication of a pressure sensor using AAO membrane with its current response under pressure is provided in Fig. 11. A pressure sensor with ultra-high sensitivity was reported. AAO membrane sandwiched between two wrinkled graphene layers acts as an insulator between two conducting graphene layers. The pores of the AAO membrane act as a pathway for current. The cyclic current response of the sensor was measured at a wide range of compressions, high compressions result in the ON state of sensors, and after removal of pressure, the sensors restore their initial state. The introduction of AAO membrane enhances sensitivity and reduces energy consumption as isolation of the graphene layers acts as an off state [130]. Few notable applications of AAO in sensing are given in Table 5 [98,106,111,115,123,126–128,130–140].

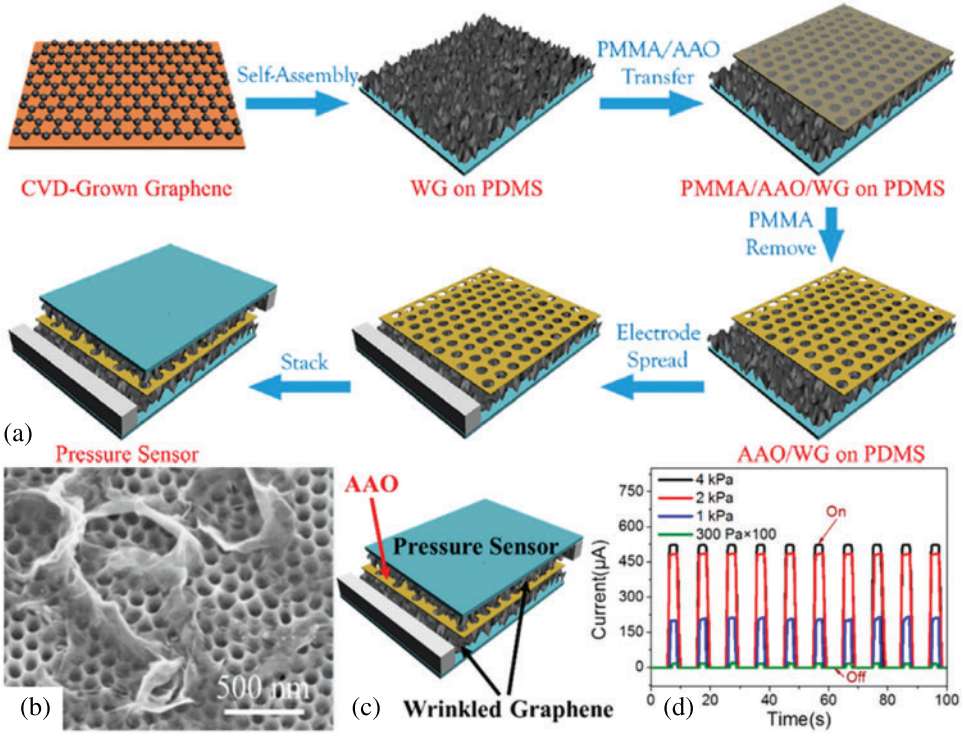

Figure 11: Ultrathin Pressure Sensors AAO membrane for insulation of two graphene layers. (a) Schematic representation of steps for fabrication process of pressure sensor, (b) SEM image of WG on AAO membrane, (c) Current response under various pressure. Reproduced from [132]. Copyright 2017 American Chemical Society

Table 5: Different types of AAO membranes for sensing applications

Membrane	Pore size (nm)	Effect of pore size	Sensor type	Application	Refs.
Au/AAO/Au	35 100	No significant effect of the pore diameter was observed	Capacitive sensor	Sensitive to He, SF_6, CO_2, N_2 and also applicable for sensing wide range of gases/vapors	[131]
AAO membranes as dust and moisture filtration interface	40 80	For increased pore size higher diffusion factor but a lower filtering performance	Optical gas sensor	CO_2 gas sensing and potential for other types of gas sensing	[111]
AAO membrane as the binder	30 300	Response time reduces as the pore diameter increases	Pressure-sensitive paint	Suitable for developing multi-layer paint systems	[130]
WG/AAO/WG	80–90	–	Pressure sensor	High-performance pressure sensor is promising for integration in flexible electronic devices to fulfill tactile sensing	[132]
Ag NPs immobilized AAO membrane	20	–	Surface enhanced Raman scattering (SERS) sensing	Potential for a multitude of applications such as process monitoring in energy generation and production, molecular adsorption and desorption during high temperature catalysis involving precious metals	[133]
Two nano-porous AAO membranes was designed to sieve exosomes	80 30	Size of exosomes is 30–100 nm in diameter porse size greater than 100nm is not effective	Isolation and quantitative analysis of exosomes	Early cancer detection	[106]

(Continued)

Table 5 (continued)

Membrane	Pore size (nm)	Effect of pore size	Sensor type	Application	Refs.
AAO filtration membranes with microfluidic channels	200	–	3-D microfluidic-channel-based electrochemical DNA biosensor	Flow-forced filtration hybridization	[115]
AAO layers on paper	40–90 40–150	Significant increase in capacitance at high humidity for sensor with larger pore size	Humidity sensors	With some treatment stable capacitance response can be obtained	[127]
Multiple AAOs by simultaneous multi-surfaces anodization (SMSA)	24.5 31.3 37.3 44.2 44.9 45.2	–	Humidity sensor	Templates and sensing applications	[128]
AAO as template for	67 110	Pore size determines NPs arrangement and interparticle distances	Plasmonic sensor	Label-free detection of DNA	[98]
AAO nanopore patterns inside the Fabry-Perot interferometer (FPI) cavity	35	–	Optical biosensor	Transparent nanostructured FPI device for highly multiplexed, label-free biodetection	[134]
Two metal films with AAO as dielectric layer	70	–	Capacitive-type touch sensor	Detection of small object such as Drosophila	[126]
Silver/AAO arrays	70	–	SERS sensors	SERS detections and many applications based on plasmon induced by 2-D silver nanoparticles encapsulated by AAO	[135]

(Continued)

Table 5 (continued)

Membrane	Pore size (nm)	Effect of pore size	Sensor type	Application	Refs.
Gold nanowire (GNW)/AAO	90	–	Metal ion sensor	Sensing electrode for applications in biochemistry and electrochemistry	[136]
AAO template	400	–	Triboelectric nanogenerator (TENG) Self-powered sensitive sensor	Real-time mobile healthcare services for the management of chronic diseases	[137]
AAO-assisted MoS_2 honeycomb structure	200	–	Humidity Sensor	Wearable sensor for multifunctional applications such as noncontact sensation of human fingertips, human breath, speech recognition, and regional sweat rate	[138]
AAO photonic crystals	30–40	–	Concentration sensor	Enhanced photoluminescence for optical devices	[139]
WO_3 deposited AAO	60	–	Metal oxide sensor	potential utilizations in the fields of energy storage devices, micro-, opto and nanoelectronics	[123]
SiO_2 coated AAO	74 65 61	Greater aqueous stability for smaller pore size	Label-free optical biosensing	Applicable for highly sensitive and specific biomolecular interaction detection	[140]

3.3.2 Prospects of AAO Membrane in Sensors

AAO membranes have promising prospects in sensing applications. High sensitivity and outstanding sensing performance of AAO membranes have been reported. Further progress in superior sensing performance is expected through structural improvement and chemical modification. AAO based implantable biosensors can be explored to be used as immunosensors for biological systems monitoring. So, miniaturized and integrated lab on chip systems based on AAO membranes may further develop sensing applications. For further advances in AAO based sensing and biosensing devices, bio-diagnostics and environmental toxic agent detection are the main focus areas.

3.4 AAO Membrane in Drug Delivery

3.4.1 Applications of AAO Membrane in Drug Delivery

A drug delivery system aims to deliver a definite amount of medicine to a specific location at a precise time [141,142]. This method helps in the targeted medication delivery, but the system's main challenges are bypassing hepatic metabolism and constant drug release to avoid multiple doses [143]. Drug delivery systems can be categorized as osmotic and diffusion-controlled membrane systems. The osmotic system contains a semi-permeable polymeric membrane that is permeable to water but not permeable to the drug. While diffusion-controlled membranes systems work on the diffusion principle, the transport of the drug across the membrane and the thickness of the membrane determines the drug release. In this type of system, porous as well as non-porous membranes can be used [9].

The properties like chemical stability and the possibility of functionalization of membrane surface for enhanced targeted drug delivery make anodic aluminum oxide membrane an excellent candidate to be used as a drug delivery system [70]. The intracellular behavior of tubular AAO structure has been investigated to develop new pathways for AAO nanotubes to be used as drug carriers for the targeted delivery of drugs [144]. In nanomedicine, nanomaterials have gained much attention from researchers to establish reliable drug delivery systems [145]. AAO membrane can also be effectively used to form hollow nanostructures, these hollow nanostructures can be used as drug carriers after the encapsulation of drugs [146–149]. Piezoelectric nanorobots referred to as nanoeels using AAO templates have also been reported for targeted drug delivery. With the help of a magnetic field, these nanoeels could be steered to the target location for on-demand drug release [150].

Polymeric micelles as nanocarriers loaded in AAO membrane can also be used to deliver poorly soluble drugs. The deposition of ultrathin polymer film via the plasma polymerization method helps in the constant release of medication for an extended period [151]. La Flamme et al. [152] used AAO biocapsules fabricated by anodization for controlled release of insulin for immunoisolation. the study proved that cell density and capsules transport area play a vital role in the optimization of the output of the device. Kang et al. [153] fabricated AAO on stents for controlled release of 2-deoxyadenosine. The effect of pore size and diameter on the drug release was studied. The results indicated that the amount of drug released during a specified time interval was directly proportional to the pore diameter and inversely proportional to the pore depth. Simovic et al. [154] combined structural and chemical modification of the pores of AAO membrane by plasma polymer deposition. They proposed that the plasma polymer layer would help control the diameter of pores at the surface of the membrane hence resulting in controlled drug release. It was concluded that the plasma polymerization reduced pore size at the surface and helped modify the physical and chemical properties. This method provides enormous flexibility for fine-tuning the drug release. In a study [155], the effect pore diameter and pore depth of AAO membrane for drug release of Paclitex, a drug used in cancer chemotherapy. The results showed that the diameter of the pores does not affect. However, pore depth has a direct relation with drug release. Park et al. [156] used an AAO membrane to fabricate mesoporous silica nanorods for controlled release of the anti-cancer drug doxorubicin. The nanorods proved to be ideal for cancer treatment, and the addition of Na content to the nanorods results in increased biodegradation speed of the nanorods.

Fig. 12 presents a schematic of drug storage and release using aligned caron nanotubes embedded in AAO for the controlled release of drugs. Nanocontainers for temperature dependent drug delivery were designed by functionalizing one end of the CNTS with thermoresponsive hydrogel, and the other end was functionalized with electrophoretic paint. The functionalized CNTs were embedded in uniform pores of AAO. Fluorescein molecules were stored in nanocontainers, and unidirectional

release from the containers below 32°C was observed. The functionalized VACNTS embedded in AAO pores has the potential to be used as drug containers and temperature-dependent controlled drug delivery [157]. Chitosan functionalized AAO membrane for the formation of drug release system with the schematic and experimental setup is provided in Fig. 13. Therapeutics releasing system was proposed by C. S. Law. For nanocontainers' formation, the surface of Al nanowires was anodized and coated with chitosan, a biocompatible polymer. The nanopores were filled with bovine serum albumin molecules labeled with fluorescein. A series of experiments were performed under static and dynamic conditions to study the therapeutic release from the nanocontainers. The effect of temperature on drug release under static condiction and dynamic conditions is presented in Figs. 10i and 10j. Enhanced degradation and diffusion rate of polymer molecules result in a much slower release under static conditions [158]. Various applications of AAO membrane in drug delivery systems are given in Table 6 [100,151,154–168].

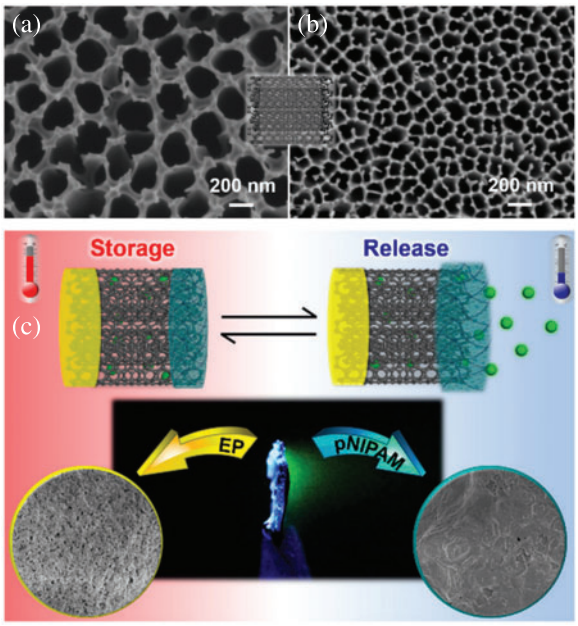

Figure 12: Modified VACNTs embedded in AAO for controlled drug release, SEM images of (a) top and (b) bottom parts of VACNTs inside the AAO membrane, (c) Schematic illustration of fluorescein storage and release mechanism from Electrophoretic paint (EP) at right and poly(N-isopropylacrylamide) (pNIPAM) at left and optical image of fluorescein released as a function of time at center. Reproduced from [157]. Copyright 2020 American Chemical Society

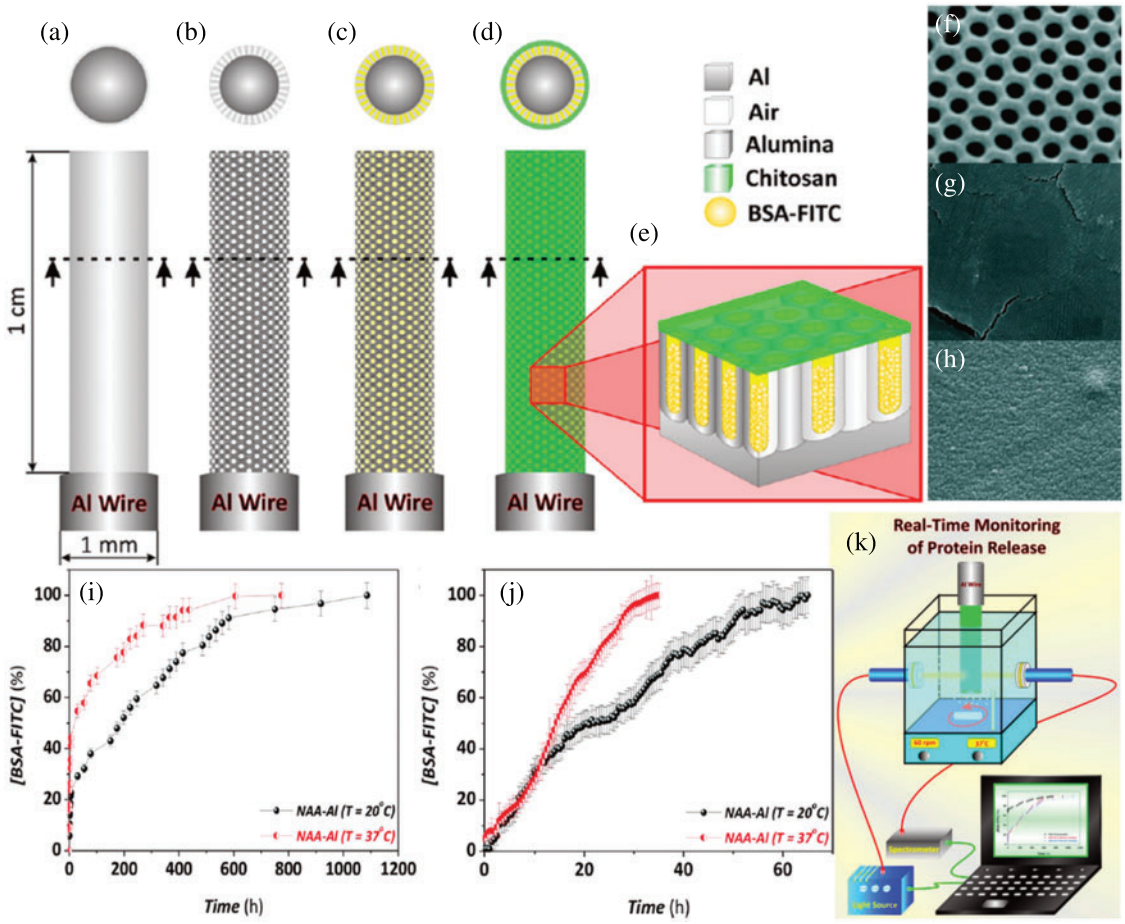

Figure 13: Therapeutics releasing AAO nanowires. Schematic representation of proposed therapeutic releasing system formation (a) electopolished Al wire, (b) after anodization (c) after protein loading (d) after chitosan coating, (e) cross sectional view, (f) SEM of nanoporous AAO-Al wire after pore widening (scale bar = 250 nm), (g) top view of NAA-Al wire after 1 cycle of chitosan coating) (scale bar = 1 μm), (h) top view of Nanoporous AAO-Al wire after 5 cycles of chitosan coating (scale bar = 1μm), effect of temperature on protein release performance from chitosan-coated NAA-Al wires under static (i) and dynamic conditions (j), (k) schematic of experimental setup to check therapeutic releasing performance. Reproduced from [158]. Copyright 2015 American Chemical Society

Table 6: AAO membranes for drug delivery

Membrane type	Pore diameter (nm)	Pore length (μm)	Drug loaded	Efficiency/ behavior of drug release	Application	Refs.
Plasma polymerized nanotubular AAO membrane	65–160	20	Indomethacin and fluorescent dye loaded in polymeric micelles	31%–55% drug release in 6–8 h followed by the slow release over 8 to 22 days	Porous therapeutic implants for an extended elution time	[151]
Electrically responsive AAO membrane electropolymerized by polypyrrole doped with the dodecylbenzenesulfonate anions (PPy/DBS)	410	60	Fluorescein isothiocyanate labelled Bovine serum albumin molecules (FITC-BSA) in 0.1 M NaDBS aqueous solution	On demand drug release with switching time less than 10 s	Pulsatile drug release for metabolic syndrome and hormone related disease	[159]
AAO with embedded silica nanotubes	20	30	A racemic mixture of the RS and SR enantiomers was used as feed solution	30 nanomoles/ 15 h	Enantiomeric drug separation	[100]
PGMA nanotubes embedded inside AAO nanopores	200	60	Doxorubicin (DOX)	67.47% and 43.66% released after 11 h for long and fragmented NTs respectively	Diagnostics and Therapeutics for cancer	[160]
Silica deposited AAO template	123	4	Prepolymer solution with DOX	–	Composite silica nanotest tubes for targeted cancer therapy	[161]

(Continued)

Table 6 (continued)

Membrane type	Pore diameter (nm)	Pore length (μm)	Drug loaded	Efficiency/ behavior of drug release	Application	Refs.
AAO nanotube structure	20	38	1 ml of 1% amoxicillin in phosphate buffered solution (PBS) was loaded	Burst effect in the first hour with ~13 μg of drug release with sustained release of 2 μg for 5 weeks	Potential for therapeutic surface coatings on medical implants	[162]
Silicone elastomer polydimethyl-siloxane (PDMS)-based contact lens with AAO thin films in central region	140	2	Timolol was mixed with a fluorescein dye loaded into the nanopores of AAO	90% of the drug was released after 30 days	Contact lens device for Glaucoma diagnostics and *in situ* drug delivery	[163]
Nanoporous AAO membrane	70	10	Se with chitosan and indomethacin	Cumulative mass release of 0.16 mg after 300 h	Promising alternatives for localized delivery of Se using simple and low-cost drug-releasing implants	[164]
AAO as template for mesoporous silica nanorods	200	50	DOX loaded in silica nanorods	Initial burst was observed within the first 24 h and was linearly released (40 μg) until the 8th day of incubation	Anti-Cancer	[156]
TiO_2 coated AAO	40–50	0.5	Paclitaxel was loaded in AAO	23 μg released in 8 days with linear increase	Cancer chemotherapy	[155]

(Continued)

Table 6 (continued)

Membrane type	Pore diameter (nm)	Pore length (μm)	Drug loaded	Efficiency/ behavior of drug release	Application	Refs.
Plasma polymerized AAO	80–90	20	Vancomycin was used as a model drug	~100% in 500 h	Fine-tuned drug release platforms to various types of drugs and applications	[154]
Aluminum wires featuring nanoporous anodic alumina layers and chitosan coatings	50	62	BSA-FITC is selected as a model drug	Sustained release performance for up to 6.5 weeks	Potential platform for future clinical therapies based on localized release of therapeutics	[158]
Electrically gated AAO membrane	80	–	Ethacrynic acid and timolol maleate	250 μg/cm^{2}h ethacrynic acid at 2 V 40 μg/cm^{2}h timolol maleate at 2 V	Potential for treatment of ocular diseases including glaucoma	[165]
Functionalized AAO with hydrophilic and hydrophobic agents	80	–	Indomethacin	Initial "burst" effect up to 65%–75% of cumulative release in the first 3 h with sustained release upto 120 h	Excellent platform for drug delivery applications	[166]
Fragmented AAO membrane	130	–	AAO particles embedded in a polymer matrix as the fillers loaded with Ag NPs	Elution of 50 h without and 350 h with PMMA sealing	Platform for *in situ* drug release	[167]

(Continued)

Table 6 (continued)

Membrane type	Pore diameter (nm)	Pore length (μm)	Drug loaded	Efficiency/ behavior of drug release	Application	Refs.
Functionalized AAO membrane with vertically aligned carbon nanotube (VACNTs) arrays	200	60	A fluorescent dye was used as a model compound	Fluorescent molecules can be stored in the VACNTs when the temperature is above 32°C, and released when the temperature decreases below 32°C	Drug storage and delivery	[157]
Electrospun coated AAO	190	50	Indole-3-acetic acid (IAAA)	90% of IAA was released during the initial 5 h and a slow release till 24 h	Controlled drug release	[168]

3.4.2 Prospects of AAO Membrane in Drug Delivery

AAO membranes have been used for effective drug delivery, but there is still plenty of room for advancement. Drug loading inside cavities of AAO membranes can be enhanced by emphasizing stable chemistries and modified anodization procedures. Furthermore, for successful drug delivery platforms, research related to the biocompatibility of the membrane to be used for delivering therapeutics and testing several medications could be crucial. The critical point is to redirect the published work for in vivo applications. For this purpose, the drug delivery system can be integrated with sensors or microchips for sustained and targeted drug delivery. Recently a power contact lens has been reported that utilizes AAO membrane as iop sensors, drug delivery and detection of ocular diseases biomarkers [163]. Microchips for fluid transport and collection can be integrated with concentration sensors for measurement of glucose concentration.

3.5 AAO Membrane in Miscellaneous Fields

3.5.1 Applications of AAO Membrane in Miscellaneous Fields

Highly variable dimensions make AAO capable of other significant applications including optical, electrical devices and several applications in biomedical. Fabrication of liquid crystal display (LCD) panels using AAO membrane has been reported. The nanocavities of the AAO membrane were filled with liquid crystal molecules. Accurately aligned liquid crystals in AAO exhibited excellent performance to be used in an electro-optical device [169]. Gold nanoparticles deposited AAO membrane has been used to prepare plasmonic absorber with the ability to absorb a wide wavelength range. This plasmonic absorber can also be used in applications like solar steam generation [170].

Davoodi et al. [171] presented the idea of nonporous AAO usage in tissue culture, biofunctionalization, drug delivery, and biosensing. Cyclic and pulse anodization was used to get uniform pores. Moreover, AAO can also be combined with biomaterials to form a composite scaffold for greater advantage. Three AAO films have different pore sizes for application as nano topological apparatuses in disease research. Cell morphology and attributes were subject to the pore size of AAO layers. AAO-1 layers (∼22 nm) did not prompt adjusted cell morphology, though AAO-2 and AAO-3 films were instigated around. Subsequently, permeable AAO films were helpful nano topological instruments for in vivo disease research because of their capacity to incorporate natural cell adhesion and growth on the anodized aluminum oxide membrane data, dependent on the cell microenvironments. The permeable AAO films like in vivo malignant growth conditions very well may be utilized for malignant growth target treatment [172].

Electric vehicles appear to be a reasonable contender to tackle the energy deficiency issue. The issues with the current lithium-particle battery are the low energy thickness restricted by the graphite anode. Also, the development of lithium dendrites that use lithium metal as an anode will prompt serious wellbeing issues. The utilization of AAO films has been proposed to improve the presentation and the security of lithium metal batteries [173]. Aluminum and its compounds are by and large used essentially for marine and clinical applications. An essential procedure to make polyaniline/chitosan/zinc stearate superhydrophobic coatings on aluminum with a small-scale nano surface structure by polymerization of aniline and sworn statement of chitosan and zinc stearate covering is also accounted for. The superhydrophobic surface shows the most important water-repellent property, which is liable for the antiadhesion of microorganisms. Also, incredible erosion obstruction of aluminum [174]. AAO has also been reportedly used for passive radiative cooling. Silica-coated porous AAO shows perfect spectral emissivity in the atmospheric window. This proposed approach can be used for low-cost and efficient radiative coolers applications [175].

Schematic illustrations of AAO membrane for applications in miscellaneous fields like electronic packaging technologies, energy harvesting, and optoelectronics are shown in Figs. 14–16, respectively. Copper nanopillar arrays embedded in pores of the AAO membrane for electronic interconnection are shown in Fig. 14. Superior anisotropic thermal conductivity was observed by CuNPA-filled AAO film. The 3-D package of film soldered with the Copper substrate is compatible with the packaging of high-density electronic and power devices [176]. Fig. 15 represents an ion pool structured nanofluidic diode designed by sandwiching AAO between oppositely charged layers of ZIF-8 and WO_3 for excellent rectification performance. Changes in pH can affect the surface charge density of ion pool nanochannel. This pH-responsive ion pool structured membrane can be used in energy harvesting applications [177]. Carbon black nanoparticles sprayed onto the AAO membrane fabricated on the silicon substrate to form metal free absorber are illustrated in Fig. 16. The reflectivity of the metal-based plasmonic absorbers was studied. The results indicate average absorbance of 97.5% can be achieved for the wavelength range 2.5–15.3 μm. These absorbers are suitable for applications in optoelectronics and photonics [178].

Soft computing techniques have been applied by many researchers for advanced applications of AAO membrane. Patel performed numerical simulations using COMSOL Multiphysics to check whether nanomembrane could function as a vibro-active nano filter. MATLAB simulations have also been performed to optimize the pore diameter of the membrane. Researchers used ANSYS analysis to study mechanical, fluid flow properties of the membrane. The real-life conditions utilization during analysis helps estimate the results of pratical applications. These techniques may be efficient for more advanced applications with a reduction of cost of practical optimization of application [15,103,110].

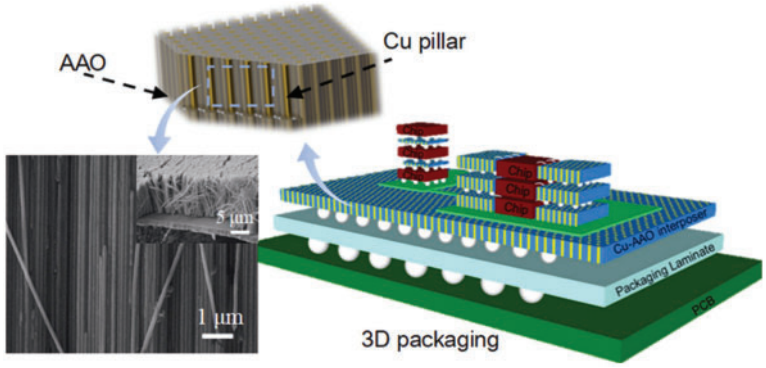

Figure 14: Schematic and SEM image of copper nanopillar array-filled AAO for anisotropic thermal conductive interconnectors. Reproduced from [176]. Copyright 2019 American Chemical Society

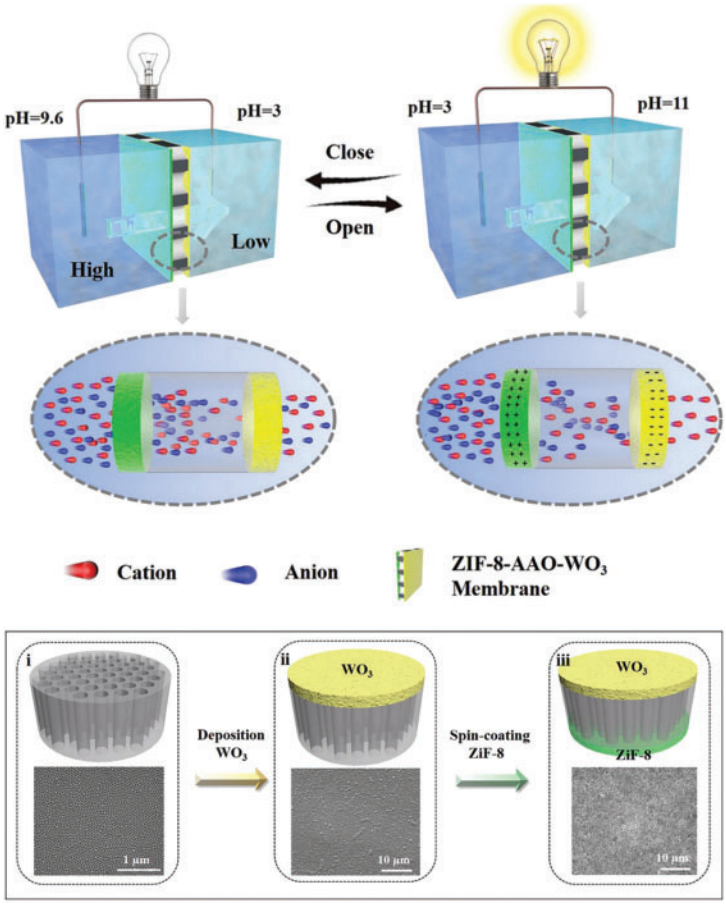

Figure 15: Schematic representation of the pH-driven Ion pool-structured multichannel gating membrane for the Osmotic energy harvesting device (top), (i–iii) SEM images with step wise fabrication description of ion pool-structured nanofluidic diode with membranes of AAO, AAO–WO_3, WO_3–AAO–ZIF-8. Reproduced from [177]. Copyright 2021 American Chemical Society

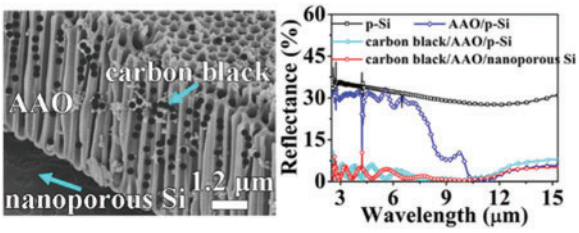

Figure 16: Carbon Black/AAO Templates on Nanoporous Si for optoelectronics and integrated photonics. SEM image of self assembled carbon black/AAO on Si (left), reflectivity of carbon black onto AAO templates on nanoporous Si (right). Reproduced from [178]. Copyright 2019 American Chemical Society

Table 7 provides applications of AAO in miscellaneous fields [57,61,65,66,94,171,176–189].

Table 7: Miscellaneous applications of AAO membranes

Membrane	Properties studied	Application	Refs.
AAO	Pore distance and length	Applications that rely upon corrosive base equilibria	[57]
AAO	Thickness	The upgraded erosion opposition	[179]
AAO	Cell adhesion and proliferation on AAO nanopore geometries and surface modifications	Nanostructured substrate for Cell development	[65]
AAO	Manipulation of chemical and structural features	Tissue Replacement	[171]
AAO	Porosity and membrane thickness	Cell culture	[180]
AAO	Porosity	Ovarian malignant growth target treatment	[172]
AAO	Controllable pore breadths, periodicity and thickness	Tissue designing applications	[66]
AAO	Porosity and surface area	Biotechnology	[181]
AAO	Hardness, impact strength, tensile and wears resistance	Automobile and aerospace	[180]
Cu nanowires on AAO	Resistive or capacitive properties	Electronic (manufacture of nanodevices) and medical services applications	[94]
AAO	Pore size	Inhibition of Lithium Dendrites by employing AAO membrane	[173]

(Continued)

Table 7 (continued)

Membrane	Properties studied	Application	Refs.
AAO	Wettability of PAN/GO nanofibers	For Li-S batteries to improve the cycle steadiness and rate limit	[183]
AAO	Investigation of polymer coatings on the surface morphology and corrosion resistance	Marine and clinical applications	[174]
AAO	Thickness	Power generation	[184]
AAO	Pore distances	High energy material science	[185]
AAO	Reactor design, synthesis conditions, the catalytic role	Wall conductivity	[186]
AAO	Surface morphologies	For surface wetting	[61]
Nafion/AAO membrane	Membrane thickness	Composite proton exchange through-plane conductivity	[187]
AAO	Structure	High chemical and thermal conductivity	[188]
AAO	Fiber structure	Water Sportage and through-plane conductivity	[189]
Cu pillars on AAO	Thermal conductivity	Electronic packaging technologies	[176]
AAO sandwiched between zeolite imidazolate framework 8 (ZIF-8) and WO_3	Rectification performance	Osmotic energy harvesting device	[177]
AAO with Carbon black nanoparticles	Light absorbance	Optoelectronic and integrated photonics	[178]

3.5.2 Prospects of AAO Membrane in Miscellaneous Fields

The prospects of AAO membrane applications translate into infinite possibilities of nanofabricated devices with enhanced properties and improved performance. Assembly of devices with enhanced properties devoted to specified application purposes, like energy and storage devices enhancing the storage capacity, can be achieved efficiently. The controllable features can be proved fruitful in the pharmaceutical, food, and energy industry. AAO based broadband absorbers can be used with other technologies for efficient thermal imaging and infrared detection. Nanochannels arrays pave the path for optimized nanofluidic diodes with applications in energy conversion zones.

4 Challenges of AAO Membranes Applications

Various challenges are associated with the application of AAO membranes. Two main types of technical challenges are worth highlighting: those related to evaluating the performance of devices and those related to scale-up under real-use conditions. Scaling up includes quality control of

mass-produced nanoscale components, consistency of component integration, impurity management. Real-use suggests testing of the effect of deviations from prescribed operating procedures. There is a gap in knowledge related to the coating of nanomaterials with anodized aluminum oxide. Exposure and toxicity make it challenging to incorporate safety parameters into early decisions or designs. For the applications of AAO incorporated nanomaterials, the production of nanomaterials is expensive, and the characterization procedure of nanomaterials is also costly. Premium materials are required to ensure the reliability of applications of the nanomaterials embedded in the AAO membrane. Solar thermal applications need hard-anodized aluminum coatings, but the challenge in implementation is that AAO coating has higher rates; the higher budget is the major problem for producing any novel innovation for the extensive application area.

Examine AAO nanopores as cell interfaces for long-term in vivo response to multiple tissues is a challenge in developing future innovative biomedical devices that incorporate. AAO based nanosensors require comprehensive testing to confirm that they are reproducible and can perform accurately in the appropriate environment. An economic and business challenge in implementing AAO nanosensors is dealing with protection and intellectual property. Manipulation of the AAO membrane-based materials is complex on the engineering and nanoscale band-gap alignments, which is advantageous for separation, generation of charge, and transportation is worthy of intensive attention in the future. Another challenge is the selection of different functional materials and assembling them toward an integrated device. In energy storage and conversion applications. For energy storage and conversion applications, methods like electrochemical deposition, physical vapor deposition, spin coating, and sol-gel [190–192] infiltration are widespread for filling or covering the AAO template with active materials. The resulting materials are not usually single crystalline. So, it is a challenge how to improve crystal quality becomes critical to reducing charge-carrier loss in crystal imperfections. Comprehensive and systematic investigations are still required to thoroughly understand the transfer dynamics of photogenerated charge carriers in the complicated surface surroundings and explore a more effective means for harnessing solar energy. However, because basic science is constantly evolving, and patent granting organizations may lack adequate functional nanotechnology expertise to evaluate applications honestly, patents create considerable barriers to product commercialization in the field of nanotechnology.

The surface of the AAO membrane has rich content of hydroxyl groups that allow them to be easily modified with the help of organic molecules according to desirable functions. Despite all these techniques used for the modification of AAO, the application of functionalized AAO membranes will depend on the unpredictable needs of the market. Yet, these techniques are only implemented by the developments in the performance of the devices and cost. This area of science and development still holds different opportunities and challenges for researchers to investigate.

5 Conclusion and Future Directions

Porous membranes with desired features resulted in the development of membrane technology. Different methods have been used for the formation of such membranes. In this paper, we have presented an overview of different methods for porous membrane formation. Different anodization methods have been used to form AAO membranes and can be used to control the geometric features of the membranes by varying the parameters. The effect of different anodization parameters on the morphology of AAO porous membrane and its properties are presented. Empirical relations defining the geometric structure parameters of porous AAO have also been recognized. Cost-effective and self-organized anodization makes it attractive for high-tech industries and biomedical applications.

Different applications reported in the literature in various fields are discussed, along with detailed applications. The following essential points can be deduced from applications of AAO.

1. The applications of AAO strongly depend on the size and chemical affinity as the membrane parameters can be controlled easily.
2. The AAO membranes can utilize all of the selectivity paradigms by modification using various molecules.
3. Effectively immobilized sensing elements within the pores can optimally interact with the analytes flowing through the pores due to the large surface-to-volume ratio of the nanopores.
4. Nanochannels of AAO promote the transfer of matter. In the presence of a barrier layer, the nanopores mimic nanocavities for containing medicine for targeted release or formation of various nanostructures with multiple applications.
5. Proper functionalizing of the surface properties and defined geometry of porous AAO can further expand its applications, resulting in up-and-coming prospects for nanotechnology applications of porous AAO membranes.

The highly variable dimensions of AAO membranes make them capable of being used in many applications. However, depending on the unpredictable requirements, there are many challenges to overcome for AAO to be used commercially. More efforts are required to improve existing methods of functionalization of membrane and the development of effectual techniques for the development of desired nanostructures using AAO. Enhanced stability and durability with improved methods may open new paths for promising applications.

Acknowledgement: This article is a part of Ph.D. thesis of Saher Manzoor. **S. Manzoor:** Draft writing; **M. W. Ashraf & S. Tayyaba:** Guidance and writing help; **M. I. Tariq & M. K. Hossain:** Reviewing and editing.

Funding Statement: The authors received no financial support for the research of this article.

Conflicts of Interest: The authors declare that they have no competing interests.

References

1. Michaels, A. (1990). Membranes, membrane processes, and their applications: Needs, unsolved problems, and challenges of the 1990's. *Desalination, 77,* 5–34. DOI 10.1016/0011-9164(90)85018-6.
2. Cadotte, J. E. (1985). Evolution of composite reverse osmosis membranes. *ACS Symposium Series, 269,* 273–294. DOI 10.1021/bk-1985-0269.ch012.
3. Petersen, R. J. (1993). Composite reverse osmosis and nanofiltration membranes. *Journal of Membrane Science, 83(1),* 81–150. DOI 10.1016/0376-7388(93)80014-O.
4. Norman, N. L., Anthony, G. F., Winston Ho, W. S. T. M. (2011). *Advanced membrane technology and applications*. New York: John Wiley & Sons.
5. Lee, K. P., Arnot, T. C., Mattia, D. (2011). A review of reverse osmosis membrane materials for desalination—Development to date and future potential. *Journal of Membrane Science, 370(1–2),* 1–22. DOI 10.1016/j.memsci.2010.12.036.
6. Adiga, S. P., Jin, C., Curtiss, L. A., Monteiro-Riviere, N. A., Narayan, R. J. (2009). Nanoporous membranes for medical and biological applications. *WIREs Nanomedicine and Nanobiotechnology, 1(5),* 568–581. DOI 10.1002/wnan.50.

7. Hossen, S., Hossain, M. K., Basher, M. K., Mia, M. N. H., Rahman, M. T. et al. (2019). Smart nanocarrier-based drug delivery systems for cancer therapy and toxicity studies: A review. *Journal of Advanced Research, 15,* 1–18. DOI 10.1016/j.jare.2018.06.005.
8. Mahfuz, A. M. U. B., Hossain, M. K., Khan, M. I., Hossain, I., Anik, M. I. (2023). Chapter 2: Smart drug-delivery nanostructured systems for cancer therapy. In: Gonçalves, G. (Ed.), *New trends in smart nanostructured biomaterials in health sciences*. Amsterdam, Netherlands: Elsevier.
9. Stamatialis, D. F., Papenburg, B. J., Gironés, M., Saiful, S., Bettahalli, S. N. M. et al. (2008). Medical applications of membranes: Drug delivery, artificial organs and tissue engineering. *Journal of Membrane Science, 308(1–2),* 1–34. DOI 10.1016/j.memsci.2007.09.059.
10. Bhadra, M., Mitra, S. (2013). Nanostructured membranes in analytical chemistry. *TrAC Trends in Analytical Chemistry, 45,* 248–263. DOI 10.1016/j.trac.2012.12.010.
11. Dineshkumar, V., Ramaswamy, D. (2017). Review on membrane technology applications in food and dairy processing. *Journal of Applied Biotechnology & Bioengineering, 3(5),* 399–407. DOI 10.15406/jabb.2017.03.00077.
12. Itaya, K., Sugawara, S., Arai, K., Saito, S. (1984). Properties of porous anodic aluminum oxide films as membranes. *Journal of Chemical Engineering of Japan, 17(5),* 514–520. DOI 10.1252/jcej.17.514.
13. Leenaars, A. F. M., Keizer, K., Burggraaf, A. J. (1984). The preparation and characterization of alumina membranes with ultra-fine pores. *Journal of Materials Science, 19(4),* 1077–1088. DOI 10.1007/BF01120016.
14. Rehman, A. U. R., Ashraf, M. W., Tayyaba, S., Bashir, M., Wasim, M. F. et al. (2021). Synthesis and growth of bismuth ferrite ($BiFeO_3$) with lanthanum (La) and yttrium (Y) doped nano-structures on anodic aluminum oxide (AAO) template. *Digest Journal of Nanomaterials and Biostructures, 16(1),* 231–238.
15. Ashraf, M. W., Manzoor, S., Shahzad Sarfraz, M., Wasim, M. F., Ali, B. et al. (2020). Fabrication and fuzzy analysis of AAO membrane with manipulated pore diameter for applications in biotechnology. *Journal of Intelligent & Fuzzy Systems, 38(5),* 5857–5864. DOI 10.3233/JIFS-179673.
16. Attiq-ur-rehman, Ashraf, M. W., Tayyaba, S., Ali, S. M., Ramay, S. M. et al. (2019). $BiFeO_3$ and La doped $BiFeO_3$ nano-particles decorated anodic Al_2O_3 porous template fabricated with two step anodization. *Materials Letters, 244,* 115–118. DOI 10.1016/j.matlet.2019.02.061.
17. Akhlaq, M., Manzoor, S., Tayyaba, S., Ashraf, M. W., Asif, A. (2022). Fuzzy analysis, fabrication and characterization of nano-porous anodic aluminum oxide membrane for Bio-MEMS. In: *Advances in intelligent data analysis and applications*, pp. 341–353. Singapore: Springer.
18. Wielage, B., Alisch, G., Lampke, T., Nickel, D. (2008). Anodizing–A key for surface treatment of aluminium. *Key Engineering Materials, 384,* 263–281. DOI 10.4028/www.scientific.net/KEM.384.263.
19. Hossain, M. K., Khan, M. I., El-Denglawey, A. (2021). A review on biomedical applications, prospects, and challenges of rare earth oxides. *Applied Materials Today, 24,* 101104. DOI 10.1016/j.apmt.2021.101104.
20. Hossain, M. K., Ahmed, M. H., Khan, M. I., Miah, M. S., Hossain, S. (2021). Recent progress of rare earth oxides for sensor, detector, and electronic device applications: A review. *ACS Applied Electronic Materials, 3(10),* 4255–4283. DOI 10.1021/acsaelm.1c00703.
21. Guy Dunstan Bengough, J. M. S. (1923). Improved process of protecting surfaces of aluminium of aluminium alloys. https://worldwide.espacenet.com/patent/search/family/010136061/publication/GB223994A?q=pn%3DGB223994A.
22. Tsyntsaru, N. (2016). Porous anodized aluminium oxide: Application outlooks. *Chemija, 27(1),* 17–23.
23. Sulka, G. D. (2008). Highly ordered anodic porous alumina formation by self-organized anodizing. In: *Nanostructured materials in electrochemistry*, pp. 1–116. Weinheim, Germany: Wiley-VCH Verlag GmbH & Co. KGaA.
24. Zhou, F. (2011). *Growth mechanism of porous anodic films on aluminium*. Manchester: University of Manchester.

25. Poinern, G. E. J., Ali, N., Fawcett, D. (2011). Progress in nano-engineered anodic aluminum oxide membrane development. *Materials, 4(3),* 487–526. DOI 10.3390/ma4030487.
26. Lee, W., Park, S. J. (2014). Porous anodic aluminum oxide: Anodization and templated synthesis of functional nanostructures. *Chemical Reviews, 114(15),* 7487–7556. DOI 10.1021/cr500002z.
27. Wu, Z., Richter, C., Menon, L. (2007). A study of anodization process during pore formation in nanoporous alumina templates. *Journal of the Electrochemical Society, 154(1),* E8. DOI 10.1149/1.2382671.
28. Larbot, A., Alary, J. A., Guizard, C., Cot, L., Gillot, J. (1987). New inorganic ultrafiltration membranes: Preparation and characterisation. *International Journal of High Technology Ceramics, 3(2),* 143–151. DOI 10.1016/0267-3762(87)90034-8.
29. Saha, S. (1994). Preparation of alumina by sol–gel process, its structures and properties. *Journal of Sol–Gel Science and Technology, 3(2),* 117–126. DOI 10.1007/BF00486718.
30. Yoldas, B. E. (1975). Alumina gels that form porous transparent Al_2O_3. *Journal of Materials Science, 10(11),* 1856–1860. DOI 10.1007/BF00754473.
31. Ksapabutr, B., Gulari, E., Wongkasemjit, S. (2004). Sol–gel transition study and pyrolysis of alumina-based gels prepared from alumatrane precursor. *Colloids and Surfaces A: Physicochemical and Engineering Aspects, 233(1–3),* 145–153. DOI 10.1016/j.colsurfa.2003.11.019.
32. Leenaars, A. F. M., Burggraaf, A. J. (1985). The preparation and characterization of alumina membranes with ultra-fine pores. *Journal of Membrane Science, 24(3),* 245–260. DOI 10.1016/S0376-7388(00)82243-7.
33. Lee, W., Ji, R., Gösele, U., Nielsch, K. (2006). Fast fabrication of long-range ordered porous alumina membranes by hard anodization. *Nature Materials, 5(9),* 741–747. DOI 10.1038/nmat1717.
34. Shingubara, S., Morimoto, K., Sakaue, H., Takahagi, T. (2004). Self-organization of a porous alumina nanohole array using a sulfuric/oxalic acid mixture as electrolyte. *Electrochemical and Solid-State Letters, 7(3),* E15. DOI 10.1149/1.1644353.
35. Sacchi, F. (1964). Recent research on anodizing and its practical implications. *Transactions of the IMF, 42(1),* 14–21. DOI 10.1080/00202967.1964.11869906.
36. Rahmanda, H., Tanaka, H., Baba, N. (1990). Preparation of porous material by replacing microstructure of anodic alumina film with metal. *Chemistry Letters, 19(4),* 621–622. DOI 10.1246/cl.1990.621.
37. Masuda, H., Satoh, M. (1996). Fabrication of gold nanodot array using anodic porous alumina as an evaporation mask. *Japanese Journal of Applied Physics, 35(1B),* L126–L129. DOI 10.1143/JJAP.35.L126.
38. Kushwaha, M. K. (2014). A comparative study of different electrolytes for obtaining thick and well-ordered nano-porous anodic aluminium oxide (AAO) films. *Procedia Materials Science, 5(3),* 1266–1273. DOI 10.1016/j.mspro.2014.07.438.
39. Tu, G. C., Huang, L. Y. (1987). Hard anodizing of 2024 aluminium alloy using pulsed DC and AC power. *Transactions of the IMF, 65(1),* 60–66. DOI 10.1080/00202967.1987.11870772.
40. Lee, W., Schwirn, K., Steinhart, M., Pippel, E., Scholz, R. et al. (2008). Structural engineering of nanoporous anodic aluminium oxide by pulse anodization of aluminium. *Nature Nanotechnology, 3(4),* 234–239. DOI 10.1038/nnano.2008.54.
41. Losic, D., Lillo, M., Losic, D. (2009). Porous alumina with shaped pore geometries and complex pore architectures fabricated by cyclic anodization. *Small, 5(12),* 1392–1397. DOI 10.1002/smll.200801645.
42. Bal, V., Awitor, K. O., Massard, C., Feschet-Chassot, E., Bokalawela, R. S. P. et al. (2012). Nanoporous surface wetting behavior: The line tension influence. *Langmuir, 28(30),* 11064–11071. DOI 10.1021/la301201k.
43. Masu, G. D., Parkoła, K. G. (2006). Anodising potential influence on well-ordered nanostructures formed by anodisation of aluminium in sulphuric acid. *Thin Solid Films, 515(1),* 338–345. DOI 10.1016/j.tsf.2005.12.094.

44. Sulka, G. D., Hnida, K. (2012). Distributed Bragg reflector based on porous anodic alumina fabricated by pulse anodization. *Nanotechnology, 23(7),* 075303. DOI 10.1088/0957-4484/23/7/075303.
45. Schwirn, K., Lee, W., Hillebrand, R., Steinhart, M., Nielsch, K. et al. (2008). Self-ordered anodic aluminum oxide formed by H_2SO_4 hard anodization. *ACS Nano, 2(2),* 302–310. DOI 10.1021/nn7001322.
46. Furneaux, R. C., Rigby, W. R., Davidson, A. P. (1989). The formation of controlled-porosity membranes from anodically oxidized aluminium. *Nature, 337(6203),* 147–149. DOI 10.1038/337147a0.
47. Zaraska, L., Sulka, G. D., Jaskuła, M. (2010). The effect of n-alcohols on porous anodic alumina formed by self-organized two-step anodizing of aluminum in phosphoric acid. *Surface and Coatings Technology, 204(11),* 1729–1737. DOI 10.1016/j.surfcoat.2009.10.051.
48. Buijnsters, J. G., Zhong, R., Tsyntsaru, N., Celis, J. P. (2013). Surface wettability of macroporous anodized aluminum oxide. *ACS Applied Materials & Interfaces, 5(8),* 3224–3233. DOI 10.1021/am4001425.
49. Lee, W., Kim, J. C., GÃsele, U. (2010). Spontaneous current oscillations during hard anodization of aluminum under potentiostatic conditions. *Advanced Functional Materials, 20(1),* 21–27. DOI 10.1002/adfm.200901213.
50. Rahman, M., Garcia-Caurel, E., Santos, A., Marsal, L. F., Pallarès, J. et al. (2012). Effect of the anodization voltage on the pore-widening rate of nanoporous anodic alumina. *Nanoscale Research Letters, 7(1),* 474. DOI 10.1186/1556-276X-7-474.
51. Ferré-Borrull, J., Rahman, M. M., Pallarès, J., Marsal, L. F. (2014). Tuning nanoporous anodic alumina distributed-Bragg reflectors with the number of anodization cycles and the anodization temperature. *Nanoscale Research Letters, 9(1),* 416. DOI 10.1186/1556-276X-9-416.
52. Chung, C. K., Zhou, R. X., Liu, T. Y., Chang, W. T. (2009). Hybrid pulse anodization for the fabrication of porous anodic alumina films from commercial purity (99%) aluminum at room temperature. *Nanotechnology, 20(5),* 055301. DOI 10.1088/0957-4484/20/5/055301.
53. Sulka, G. D., Parkoła, K. G. (2007). Temperature influence on well-ordered nanopore structures grown by anodization of aluminium in sulphuric acid. *Electrochimica Acta, 52(5),* 1880–1888. DOI 10.1016/j.electacta.2006.07.053.
54. Kozhukhova, A. E., du Preez, S. P., Bessarabov, D. G. (2019). Preparation of anodized aluminium oxide at high temperatures using low purity aluminium (Al6082). *Surface and Coatings Technology, 378(2),* 124970. DOI 10.1016/j.surfcoat.2019.124970.
55. Erdogan, P., Yuksel, B., Birol, Y. (2012). Effect of chemical etching on the morphology of anodic aluminum oxides in the two-step anodization process. *Applied Surface Science, 258(10),* 4544–4550. DOI 10.1016/j.apsusc.2012.01.025.
56. Ateş, S., Baran, E., Yazıcı, B. (2018). The nanoporous anodic alumina oxide formed by two-step anodization. *Thin Solid Films, 648(2018),* 94–102. DOI 10.1016/j.tsf.2018.01.013.
57. Kovaleva, E. G., Molochnikov, L. S., Tambasova, D., Marek, A., Chestnut, M. et al. (2020). Electrostatic properties of inner nanopore surfaces of anodic aluminum oxide membranes upon high temperature annealing revealed by EPR of pH-sensitive spin probes and labels. *Journal of Membrane Science, 604,* 118084. DOI 10.1016/j.memsci.2020.118084.
58. Yang, J., Wang, J., Wang, C. W., He, X., Li, Y. et al. (2014). Intermediate wetting states on nanoporous structures of anodic aluminum oxide surfaces. *Thin Solid Films, 562,* 353–360. DOI 10.1016/j.tsf.2014.04.020.
59. Zhang, H., Yin, L., Shi, S., Liu, X., Wang, Y. et al. (2015). Facile and fast fabrication method for mechanically robust superhydrophobic surface on aluminum foil. *Microelectronic Engineering, 141(3),* 238–242. DOI 10.1016/j.mee.2015.03.048.
60. Ye, J., Yin, Q., Zhou, Y. (2009). Superhydrophilicity of anodic aluminum oxide films: From "honeycomb" to "bird's" nest. *Thin Solid Films, 517(21),* 6012–6015. DOI 10.1016/j.tsf.2009.04.042.

61. Zhang, W., Huang, L., Zi, C., Cai, Y., Zhang, Y. et al. (2018). Wettability of porous anodic aluminium oxide membranes with three-dimensional, layered nanostructures. *Journal of Porous Materials, 25(6),* 1707–1714. DOI 10.1007/s10934-018-0584-5.
62. Ko, S., Lee, D., Jee, S., Park, H., Lee, K. et al. (2006). Mechanical properties and residual stress in porous anodic alumina structures. *Thin Solid Films, 515(4),* 1932–1937. DOI 10.1016/j.tsf.2006.07.169.
63. Sundararajan, M., Devarajan, M., Jaafar, M. (2020). Investigation of surface and mechanical properties of anodic aluminium oxide (AAO) developed on Al substrate for an electronic package enclosure. *Surface and Coatings Technology, 401(12),* 126273. DOI 10.1016/j.surfcoat.2020.126273.
64. Osmanbeyoglu, H. U., Hur, T. B., Kim, H. K. (2009). Thin alumina nanoporous membranes for similar size biomolecule separation. *Journal of Membrane Science, 343(1–2),* 1–6. DOI 10.1016/j.memsci.2009.07.027.
65. Brüggemann, D. (2013). Nanoporous aluminium oxide membranes as cell interfaces. *Journal of Nanomaterials, 2013(3),* 1–18. DOI 10.1155/2013/460870.
66. Poinern, G. E. J., Le, X. T., Hager, M., Becker, T., Fawcett, D. (2013). Electrochemical synthesis, characterisation, and preliminary biological evaluation of an anodic aluminium oxide membrane with a pore size of 100 nanometres for a potential cell culture substrate. *American Journal of Biomedical Engineering, 3(6),* 119–131. DOI 10.5923/j.ajbe.20130306.01.
67. Liu, S., Tian, J., Zhang, W. (2021). Fabrication and application of nanoporous anodic aluminum oxide: A review. *Nanotechnology, 32(22),* 222001. DOI 10.1088/1361-6528/abe25f.
68. Mao, Y., Park, T. J., Zhang, F., Zhou, H., Wong, S. S. (2007). Environmentally friendly methodologies of nanostructure synthesis. *Small, 3(7),* 1122–1139. DOI 10.1002/(ISSN)1613-6829.
69. Shaban, M., Mustafa, M., Khan, A. A. P. (2020). Hexagonal diameter in cadmium sulfide/anodic alumina nanoporous bi-layer membrane by a sol-gel spin coating and their sensing application. *Applied Physics A: Materials Science and Processing, 126(4),* 268. DOI 10.1007/s00339-020-3371-5.
70. Ruiz-Clavijo, A., Caballero-Calero, O., Martín-González, M. (2021). Revisiting anodic alumina templates: From fabrication to applications. *Nanoscale, 13(4),* 2227–2265. DOI 10.1039/D0NR07582E.
71. Li, W., Zhang, J., Shen, T., Jones, G. A., Grundy, P. J. (2011). Magnetic nanowires fabricated by anodic aluminum oxide template—A brief review. *Science China: Physics, Mechanics and Astronomy, 54(7),* 1181–1189. DOI 10.1007/s11433-011-4371-4.
72. Tomassi, P., Buczko, Z. (2015). Aluminum anodic oxide AAO as a template for formation of metal nanostructures. In: *Electroplating of nanostructures*. London, UK: InTech.
73. Yi, G., Schwarzacher, W. (1999). Single crystal superconductor nanowires by electrodeposition. *Applied Physics Letters, 74(12),* 1746–1748. DOI 10.1063/1.123675.
74. Zhang, Y., Li, G., Wu, Y., Zhang, B., Song, W. et al. (2002). Antimony nanowire arrays fabricated by pulsed electrodeposition in anodic alumina membranes. *Advanced Materials, 14(17),* 1227–1230. DOI 10.1002/1521-4095(20020903)14:17<1227::AID-ADMA1227>3.0.CO;2-2.
75. Nielsch, K., Müller, F., Li, A. P., Gösele, U. (2000). Uniform nickel deposition into ordered alumina pores by pulsed electrodeposition. *Advanced Materials, 12(8),* 582–586. DOI 10.1002/(SICI)1521-4095(200004)12:8<582::AID-ADMA582>3.0.CO;2-3.
76. Pan, H., Sun, H., Poh, C., Feng, Y., Lin, J. (2005). Single-crystal growth of metallic nanowires with preferred orientation. *Nanotechnology, 16(9),* 1559–1564. DOI 10.1088/0957-4484/16/9/025.
77. Thongmee, S., Pang, H. L., Ding, J., Yi, J. B., Lin, J. Y. (2008). Fabrication and magnetic properties of metal nanowires via AAO templates. *Journal of Magnetism and Magnetic Materials, 321(18),* 2712–2716. DOI 10.1016/j.jmmm.2009.03.074.
78. Yang, R., Sui, C., Gong, J., Qu, L. (2007). Silver nanowires prepared by modified AAO template method. *Materials Letters, 61(3),* 900–903. DOI 10.1016/j.matlet.2006.06.009.

79. Wu, Z., Zhang, Y., Du, K. (2013). A simple and efficient combined AC-DC electrodeposition method for fabrication of highly ordered Au nanowires in AAO template. *Applied Surface Science, 265,* 149–156. DOI 10.1016/j.apsusc.2012.10.154.
80. Ganapathi, A., Swaminathan, P., Neelakantan, L. (2019). Anodic aluminum oxide template assisted synthesis of copper nanowires using a galvanic displacement process for electrochemical denitrification. *ACS Applied Nano Materials, 2(9),* 5981–5988. DOI 10.1021/acsanm.9b01409.
81. Zhang, C., Lu, Y., Zhao, B., Hao, Y., Liu, Y. (2016). Facile fabrication of Ag dendrite-integrated anodic aluminum oxide membrane as effective three-dimensional SERS substrate. *Applied Surface Science, 377,* 167–173. DOI 10.1016/j.apsusc.2016.03.132.
82. Pourjafari, D., Serrano, T., Kharissov, B., Peña, Y., Gómez, I. (2015). Template assisted synthesis of poly(3-hexylthiophene) nanorods and nanotubes: Growth mechanism and corresponding band gap. *International Journal of Materials Research, 106(4),* 414–420. DOI 10.3139/146.111196.
83. Gao, X., Liu, L., Birajdar, B., Ziese, M., Lee, W. et al. (2009). High-density periodically ordered magnetic cobalt ferrite nanodot arrays by template-assisted pulsed laser deposition. *Advanced Functional Materials, 19(21),* 3450–3455. DOI 10.1002/adfm.200900422.
84. Chen, P. L., Chang, J. K., Kuo, C. T., Pan, F. M. (2004). Anodic aluminum oxide template assisted growth of vertically aligned carbon nanotube arrays by ECR-CVD. *Diamond and Related Materials, 13(11–12),* 1949–1953. DOI 10.1016/j.diamond.2004.05.007.
85. Xu, T. N., Wu, H. Z., Lao, Y. F., Qiu, D. J., Chen, N. B. et al. (2004). Anodic-aluminium-oxide template-assisted growth of ZnO nanodots on Si (100) at low temperature. *Chinese Physics Letters, 21(7),* 1327–1329. DOI 10.1088/0256-307X/21/7/040.
86. Yang, W., Oh, Y., Kim, J., Kim, H., Shin, H. et al. (2016). Photoelectrochemical properties of vertically aligned $CuInS_2$ nanorod arrays prepared via template-assisted growth and transfer. *ACS Applied Materials and Interfaces, 8(1),* 425–431. DOI 10.1021/acsami.5b09241.
87. Su, C. C., Teng, Y. C., Chang, S. H. (2010). Synthesize uniform carbon nanocoils by anodic aluminum oxide. *2010 IEEE 5th International Conference on Nano/Micro Engineered and Molecular Systems*, pp. 950–953. Xiamen, China.
88. Lai, C. H., Chang, C. W., Tseng, T. Y. (2010). Size-dependent field-emission characteristics of ZnO nanowires grown by porous anodic aluminum oxide templates assistance. *Thin Solid Films, 518(24),* 7283–7286. DOI 10.1016/j.tsf.2010.04.091.
89. Li, H., Zhang, H., Wu, H., Hao, J., Liu, C. (2020). Tree-like structures of InN nanoparticles on agminated anodic aluminum oxide by plasma-assisted reactive evaporation. *Applied Surface Science, 503,* 144309. DOI 10.1016/j.apsusc.2019.144309.
90. Maurya, M. R., Toutam, V. (2019). Fast response UV detection based on waveguide characteristics of vertically grown ZnO nanorods partially embedded in anodic alumina template. *Nanotechnology, 30(8),* 085704. DOI 10.1088/1361-6528/aaf545.
91. Liu, C. J., Chen, S. Y., Shih, L. J., Huang, H. J. (2010). Fabrication of nanotubules of thermoelectric γ-$Na_{0.7}CoO_2$ using porous aluminum oxide membrane as supporting template. *Materials Chemistry and Physics, 119(3),* 424–427. DOI 10.1016/j.matchemphys.2009.09.016.
92. Tzaneva, B. R., Naydenov, A. I., Todorova, S. ZH., Videkov, V. H., Milusheva, V. S. et al. (2016). Cobalt electrodeposition in nanoporous anodic aluminium oxide for application as catalyst for methane combustion. *Electrochimica Acta, 191,* 192–199. DOI 10.1016/j.electacta.2016.01.063.
93. Maghsodi, A., Adlnasab, L., Shabanian, M., Javanbakht, M. (2018). Optimization of effective parameters in the synthesis of nanopore anodic aluminum oxide membrane and arsenic removal by prepared magnetic iron oxide nanoparicles in anodic aluminum oxide membrane via ultrasonic-hydrothermal method. *Ultrasonics Sonochemistry, 48,* 441–452. DOI 10.1016/j.ultsonch.2018.07.003.

94. Nehra, M., Dilbaghi, A. N., Singh, V., Singhal, N. K., Kumar, S. (2020). Highly ordered and crystalline Cu nanowires in anodic aluminum oxide membranes for biomedical applications. *Physica Status Solidi (a), 217(13),* 1900842. DOI 10.1002/pssa.201900842.
95. Ghezghapan, S. M. S., Saba, M. (2018). Synthesizing high aspect ratio aluminum oxide nanowires from highly-ordered anodic self-assembled templates. https://doi.org/10.1149/osf.io/zejvp.
96. Esfandi, F., Saramad, S., Shahmirzadi, M. R. (2017). Characterizing and simulation the scintillation properties of zinc oxide nanowires in AAO membrane for medical imaging applications. *Journal of Instrumentation, 12(7),* P07004. DOI 10.1088/1748-0221/12/07/P07004.
97. Attiq-ur-rehman, Ashraf, M. W., Mahmood, A., Rehman, A. U., Ramay, S. M. et al. (2021). Growth of Zr-$BiFeO_3$ nanostructures on two step anodized porous alumina for estimation of optical and dielectric response. *Physica E: Low-Dimensional Systems and Nanostructures, 127,* 114513. DOI 10.1016/j.physe.2020.114513.
98. Lednický, T., Bonyár, A. (2020). Large scale fabrication of ordered gold nanoparticle-epoxy surface nanocomposites and their application as label-free plasmonic DNA biosensors. *ACS Applied Materials & Interfaces, 12(4),* 4804–4814. DOI 10.1021/acsami.9b20907.
99. Shi, W., Shen, Y., Ge, D., Xue, M., Cao, H. et al. (2008). Functionalized anodic aluminum oxide (AAO) membranes for affinity protein separation. *Journal of Membrane Science, 325(2),* 801–808. DOI 10.1016/j.memsci.2008.09.003.
100. Lee, S. B., Mitchell, D. T., Trofin, L., Nevanen, T. K. et al. (2002). Antibody-based bio-nanotube membranes for enantiomeric drug separations. *Science, 296(576),* 2198–2200. DOI 10.1126/science.1071396.
101. Losic, D., Cole, M. A., Dollmann, B., Vasilev, K., Griesser, H. J. (2008). Surface modification of nanoporous alumina membranes by plasma polymerization. *Nanotechnology, 19(24),* 24570. DOI 10.1088/0957-4484/19/24/245704.
102. Yamaguchi, A., Uejo, F., Yoda, T., Uchida, T., Tanamura, Y. et al. (2004). Self-assembly of a silica-surfactant nanocomposite in a porous alumina membrane. *Nature Materials, 3(5),* 337–341. DOI 10.1038/nmat1107.
103. Ashraf, M. W., Qureshi, M. Z., Ghaffar, F., Tayyaba, S. (2016). Structural study of AAO membrane during the dialysis process. *2016 International Conference on Intelligent Systems Engineering (ICISE)*, Islamabad, Pakistan.
104. Thormann, A., Berthold, L., Gšring, P., Lelonek, M., Heilmann, A. (2012). Nanoporous aluminum oxide membranes for separation and biofunctionalization. *Procedia Engineering, 44,* 1107–1111. DOI 10.1016/j.proeng.2012.08.693.
105. Khan Kasi, A., Khan Kasi, J., Afzulpurkar, N., Bohez, E., Tuantranont, A. et al. (2010). Novel anodic aluminum oxide (AAO) nanoporous membrane for wearable hemodialysis device. *International Conference on Communications and Electronics 2010*, pp. 98–101. Nha Trang, Veitnam, IEEE.
106. Chang, Y. J., Yang, W. T., Wu, J. C. (2019). Isolation and detection of exosomes via AAO membrane and QCM measurement. *Microelectronic Engineering, 216,* 111094. DOI 10.1016/j.mee.2019.111094.
107. Liu, Y., Lou, J., Ni, M., Song, C., Wu, J. et al. (2016). Bioinspired bifunctional membrane for efficient clean water generation. *ACS Applied Materials & Interfaces, 8(1),* 772–779. DOI 10.1021/acsami.5b09996.
108. Nikam, S. B., Syamakumari, A. (2020). Enantioselective separation using chiral amino acid functionalized polyfluorene coated on mesoporous anodic aluminum oxide membranes. *Analytical Chemistry, 92(10),* 6850–6857. DOI 10.1021/acs.analchem.9b04699.
109. Mahadi, H., Kasi, A. K., Kasi, J. K., Afzulpurkar, N. (2012). Anodic aluminum oxide (AAO) to AAO bonding and their application for fabrication of 3D microchannel. *Nanoscience and Nanotechnology Letters, 4(5),* 569–573(5). DOI 10.1166/nnl.2012.1354.
110. Patel, Y., Janusas, G., Palevicius, A., Vilkauskas, A. (2020). Development of nanoporous AAO membrane for nano filtration using the acoustophoresis method. *Sensors, 20(14),* 3833. DOI 10.3390/s20143833.

111. Ma, Y., Kaczynski, J., Ranacher, C., Roshanghias, A., Zauner, M. et al. (2018). Nano-porous aluminum oxide membrane as filtration interface for optical gas sensor packaging. *Microelectronic Engineering, 198(5),* 29–34. DOI 10.1016/j.mee.2018.06.013.

112. Kasi, A. K., Kasi, J. K., Hasan, M., Afzulpurkar, N., Pratontep, S. et al. (2012). Fabrication of low cost anodic aluminum oxide (AAO) tubular membrane and their application for hemodialysis. *Advanced Materials Research, 550–553,* 2040–2045. DOI 10.4028/www.scientific.net/AMR.550-553.2040.

113. Wen, F. Y., Chen, P. S., Liao, T. W., Juang, Y. J. (2018). Microwell-assisted filtration with anodic aluminum oxide membrane for Raman analysis of algal cells. *Algal Research, 33(1),* 412–418. DOI 10.1016/j.algal.2018.06.022.

114. Park, Y., Kim, S., Jang, I. H., Nam, Y. S., Hong, H. et al. (2016). Role of the electric field in selective ion filtration in nanostructures. *Analyst, 141(4),* 1294–1300. DOI 10.1039/C5AN01980J.

115. Kim, Y. J., Jones, J. E., Li, H., Yampara-Iquise, H., Zheng, G. et al. (2013). Three-dimensional (3-D) microfluidic-channel-based DNA biosensor for ultra-sensitive electrochemical detection. *Journal of Electroanalytical Chemistry, 702,* 72–78. DOI 10.1016/j.jelechem.2013.04.021.

116. Song, J., Oh, H., Kong, H., Jang, J. (2011). Polyrhodanine modified anodic aluminum oxide membrane for heavy metal ions removal. *Journal of Hazardous Materials, 187(1–3),* 311–317. DOI 10.1016/j.jhazmat.2011.01.026.

117. Kasi, A. K., Kasi, J. K., Bokhari, M. (2018). Fabrication of mechanically stable AAO membrane with improved fluid permeation properties. *Microelectronic Engineering, 187(2),* 95–100. DOI 10.1016/j.mee.2017.11.019.

118. Chang, H. C., Chen, Y. H., Lo, A. T., Hung, S. S., Lin, S. L. et al. (2014). Modified nanoporous membranes on centrifugal microfluidic platforms for detecting heavy metal ions. *Materials Research Innovations, 18(sup2),* S2-685. DOI 10.1179/1432891714Z.000000000532.

119. Kim, Y., Cha, M., Choi, Y., Joo, H., Lee, J. et al. (2013). Electrokinetic separation of biomolecules through multiple nano-pores on membrane. *Chemical Physics Letters, 561,* 63–67. DOI 10.1016/j.cplett.2013.01.018.

120. Phuong, N., Andisetiawan, A., van Lam, D., Kim, J. H., Choi, D. S. et al. (2016). Nano sand filter with functionalized nanoparticles embedded in anodic aluminum oxide templates. *Scientific Reports, 6(1),* 1–8. DOI 10.1038/srep37673.

121. Hun, C. W., Chiu, Y. J., Luo, Z., Chen, C. C., Chen, S. H. (2018). A new technique for batch production of tubular anodic aluminum oxide films for filtering applications. *Applied Sciences, 8(7),* 1055. DOI 10.3390/app8071055.

122. Santos, A., Kumeria, T., Losic, D. (2013). Nanoporous anodic aluminum oxide for chemical sensing and biosensors. *TrAC Trends in Analytical Chemistry, 44(20),* 25–38. DOI 10.1016/j.trac.2012.11.007.

123. Gorokh, G., Mozalev, A., Solovei, D., Khatko, V., Llobet, E. et al. (2006). Anodic formation of low-aspect-ratio porous alumina films for metal-oxide sensor application. *Electrochimica Acta, 52(4),* 1771–1780. DOI 10.1016/j.electacta.2006.01.081.

124. Han, N., Deng, P., Chen, J., Chai, L., Gao, H. et al. (2010). Electrophoretic deposition of metal oxide films aimed for gas sensors application: The role of anodic aluminum oxide (AAO)/Al composite structure. *Sensors and Actuators B: Chemical, 144(1),* 267–273. DOI 10.1016/j.snb.2009.10.068.

125. Lo, P. H., Hong, C., Lo, S. C., Fang, W. (2011). Implementation of inductive proximity sensor using nanoporous anodic aluminum oxide layer, *2011 16th International Solid-State Sensors, Actuators and Microsystems Conference*, Beijing, China. DOI 10.1109/transducers.2011.5969829.

126. Hong, C., Chu, L., Lai, W., Chiang, A. S., Fang, W. (2011). Implementation of a new capacitive touch sensor using the nanoporous anodic aluminum oxide (np-AAO) structure. *IEEE Sensors Journal, 11(12),* 3409–3416. DOI 10.1109/JSEN.2011.2160255.

127. Balde, M., Vena, A., Sorli, B. (2015). Fabrication of porous anodic aluminium oxide layers on paper for humidity sensors. *Sensors and Actuators B: Chemical, 220(4),* 829–839. DOI 10.1016/j.snb.2015.05.053.

128. Jeong, S. H., Im, H. L., Hong, S., Park, H., Baek, J. et al. (2017). Massive, eco-friendly, and facile fabrication of multi-functional anodic aluminum oxides: Application to nanoporous templates and sensing platforms. *RSC Advances, 7(8),* 4518–4530. DOI 10.1039/C6RA25201J.

129. Kumeria, T., Kurkuri, M., Diener, K., Zhang, C., Parkinson, L. et al. (2011). Reflectometric interference biosensing using nanopores. *Integration Into Microfluidics, 8204,* 82043C. DOI 10.1117/12.903217.

130. Chen, W., Gui, X., Liang, B., Yang, R., Zheng, Y. et al. (2017). Structural engineering for high sensitivity, ultrathin pressure sensors based on wrinkled graphene and anodic aluminum oxide membrane. *ACS Applied Materials & Interfaces, 9(28),* 24111–24117. DOI 10.1021/acsami.7b05515.

131. Podgolin, S. K., Petukhov, D. I., Dorofeev, S. G., Eliseev, A. A. (2020). Anodic alumina membrane capacitive sensors for detection of vapors. *Talanta, 219,* 121248. DOI 10.1016/j.talanta.2020.121248.

132. Peng, D., Chen, J., Jiao, L., Liu, Y. (2018). A fast-responding semi-transparent pressure-sensitive paint based on through-hole anodized aluminum oxide membrane. *Sensors and Actuators A: Physical, 274(2),* 10–18. DOI 10.1016/j.sna.2018.02.026.

133. Pinkhasova, P., Chen, H., Verhoeven, T. M. W. G. M., Sukhishvili, S. (2013). Thermally annealed Ag nanoparticles on anodized aluminium oxide for SERS sensing. *RSC Advances, 3(39),* 17954. DOI 10.1039/c3ra43808b.

134. He, Y., Li, X., Que, L. (2014). A transparent nanostructured optical biosensor. *Journal of Biomedical Nanotechnology, 10(5),* 767–774. DOI 10.1166/jbn.2014.1769.

135. Huang, C. H., Lin, H. Y., Chen, S., Liu, C. Y., Chui, H. C. et al. (2011). Electrochemically fabricated self-aligned 2-D silver/alumina arrays as reliable SERS sensors. *Optics Express, 19(12),* 11441–11450. DOI 10.1364/OE.19.011441.

136. Umh, H. N., Shin, H. H., Yi, J., Kim, Y. (2015). Fabrication of gold nanowires (GNW) using aluminum anodic oxide (AAO) as a metal-ion sensor. *Korean Journal of Chemical Engineering, 32(2),* 299–302. DOI 10.1007/s11814-014-0201-5.

137. Song, W., Gan, B., Jiang, T., Zhang, Y., Yu, A. et al. (2016). Nanopillar arrayed triboelectric nanogenerator as a self-powered sensitive sensor for a sleep monitoring system. *ACS Nano, 10(8),* 8097–8103. DOI 10.1021/acsnano.6b04344.

138. Mondal, S., Kim, S. J., Choi, C. G. (2020). Honeycomb-like MoS_2 nanotube array-based wearable sensors for noninvasive detection of human skin moisture. *ACS Applied Materials and Interfaces, 12(14),* 17029–17038. DOI 10.1021/acsami.9b22915.

139. Wang, G., Wang, J., Li, S. Y., Zhang, J. W., Wang, C. W. (2015). One-dimensional alumina photonic crystals with a narrow band gap and their applications to high-sensitivity concentration sensor and photoluminescence enhancement. *Superlattices and Microstructures, 86,* 546–551. DOI 10.1016/j.spmi.2015.08.004.

140. Fan, Y., Ding, Y., Zhang, Y., Ma, H., He, Y. et al. (2014). A SiO_2-coated nanoporous alumina membrane for stable label-free waveguide biosensing. *RSC Advances, 4(108),* 62987–62995. DOI 10.1039/C4RA08839E.

141. Anik, M. I., Hossain, M. K., Hossain, I., Ahmed, I., Doha, R. M. (2021). Biomedical applications of magnetic nanoparticles. In: Ehrmann, A., Nguyen, T. A., Ahmadi, M., Farmani, A., Nguyen-Tri, P. (Eds.), *Magnetic nanoparticle-based hybrid materials*, 1st edition, pp. 463–497. Sawston, UK: Elsevier.

142. Anik, M. I., Hossain, M. K., Hossain, I., Mahfuz, A. M. U. B., Rahman, M. T. et al. (2021). Recent progress of magnetic nanoparticles in biomedical applications: A review. *Nano Select, 2(6),* 1146–1186. DOI 10.1002/nano.202000162.

143. Gupta Manish, S. V. (2011). Targeted drug delivery system: A review. *Research Journal of Chemical Sciences, 2(1),* 135–138.

144. Sun, X., Jiang, L., Wang, C., Sun, S., Mei, L. et al. (2019). Systematic investigation of intracellular trafficking behavior of one-dimensional alumina nanotubes. *Journal of Materials Chemistry B, 7(12),* 2043–2053. DOI 10.1039/C8TB03349H.

145. Li, L., Chen, D., Zhang, Y., Deng, Z., Ren, X. et al. (2007). Magnetic and fluorescent multifunctional chitosan nanoparticles as a smart drug delivery system. *Nanotechnology, 18(40),* 405102. DOI 10.1088/0957-4484/18/40/405102.

146. Hou, P., Liu, C., Shi, C., Cheng, H. (2012). Carbon nanotubes prepared by anodic aluminum oxide template method. *Chinese Science Bulletin, 57(2–3),* 187–204. DOI 10.1007/s11434-011-4892-2.

147. Losic, D., Simovic, S. (2009). Self-ordered nanopore and nanotube platforms for drug delivery applications. *Expert Opinion on Drug Delivery, 6(12),* 1363–1381. DOI 10.1517/17425240903300857.

148. Sinn Aw, M., Kurian, M., Losic, D. (2014). Non-eroding drug-releasing implants with ordered nanoporous and nanotubular structures: Concepts for controlling drug release. *Biomaterials Science, 2(1),* 10–34. DOI 10.1039/C3BM60196J.

149. Yin, J., Cui, Y., Yang, G., Wang, H. (2010). Molecularly imprinted nanotubes for enantioselective drug delivery and controlled release. *Chemical Communications, 46(41),* 7688. DOI 10.1039/c0cc01782e.

150. Mushtaq, F., Torlakcik, H., Hoop, M., Jang, B., Carlson, F. et al. (2019). Motile piezoelectric nanoeels for targeted drug delivery. *Advanced Functional Materials, 29(12),* 1808135. DOI 10.1002/adfm.201808135.

151. Aw, M. S., Simovic, S., Addai-Mensah, J., Losic, D. (2011). Polymeric micelles in porous and nanotubular implants as a new system for extended delivery of poorly soluble drugs. *Journal of Materials Chemistry, 21(20),* 7082–7089. DOI 10.1039/c0jm04307a.

152. La Flamme, K. E., Latempa, T. J., Grimes, C. A., Desai, T. A. (2007). The effects of cell density and device arrangement on the behavior of macroencapsulated β-cells. *Cell Transplantation, 16(8),* 765–774. DOI 10.3727/000000007783465262.

153. Kang, H. J., Kim, D. J., Park, S. J., Yoo, J. B., Ryu, Y. S. (2007). Controlled drug release using nanoporous anodic aluminum oxide on stent. *Thin Solid Films, 515(12),* 5184–5187. DOI 10.1016/j.tsf.2006.10.029.

154. Simovic, S., Losic, D., Vasilev, K. (2010). Controlled drug release from porous materials by plasma polymer deposition. *Chemical Communications, 46(8),* 1317. DOI 10.1039/b919840g.

155. Kwak, D. H., Yoo, J. B., Kim, D. J. (2010). Drug release behavior from nanoporous anodic aluminum oxide. *Journal of Nanoscience and Nanotechnology, 10(1),* 345–348. DOI 10.1166/jnn.2010.1531.

156. Park, S. B., Joo, Y. H., Kim, H., Ryu, W., Park, Y. I. (2015). Biodegradation-tunable mesoporous silica nanorods for controlled drug delivery. *Materials Science and Engineering C, 50(3475),* 64–73. DOI 10.1016/j.msec.2015.01.073.

157. Niamlaem, M., Phuakkong, O., Garrigue, P., Goudeau, B., Ravaine, V. et al. (2020). Asymmetric modification of carbon nanotube arrays with thermoresponsive hydrogel for controlled delivery. *ACS Applied Materials and Interfaces, 12(20),* 23378. DOI 10.1021/acsami.0c01017.

158. Law, C. S., Santos, A., Kumeria, T., Losic, D. (2015). Engineered therapeutic-releasing nanoporous anodic alumina-aluminum wires with extended release of therapeutics. *ACS Applied Materials and Interfaces, 7(6),* 3846–3853. DOI 10.1021/am5091963.

159. Jeon, G., Yang, S. Y., Byun, J., Kim, J. K. (2011). Electrically actuatable smart nanoporous membrane for pulsatile drug release. *Nano Letters, 11(3),* 1284–1288. DOI 10.1021/nl104329y.

160. Chen, G., Chen, R., Zou, C., Yang, D., Chen, Z. S. (2014). Fragmented polymer nanotubes from sonication-induced scission with a thermo-responsive gating system for anti-cancer drug delivery. *Journal of Materials Chemistry B, 2(10),* 1327–1334. DOI 10.1039/C3TB21512A.

161. Buyukserin, F., Altuntas, S., Aslim, B. (2014). Fabrication and modification of composite silica nano test tubes for targeted drug delivery. *RSC Advances, 4(45),* 23535–23539. DOI 10.1039/C4RA00871E.

162. Noh, K., Brammer, K. S., Choi, C., Kim, S. H., Frandsen, C. J. et al. (2011). A new nano-platform for drug release via nanotubular aluminum oxide. *Journal of Biomaterials and Nanobiotechnology, 2(3),* 226–233. DOI 10.4236/jbnb.2011.23028.

163. Song, C., Ben-Shlomo, G., Que, L. (2019). A multifunctional smart soft contact lens device enabled by nanopore thin film for glaucoma diagnostics and *in situ* drug delivery. *Journal of Microelectromechanical Systems, 28(5),* 810–816. DOI 10.1109/JMEMS.2019.2927232.

164. Saji, V. S., Kumeria, T., Gulati, K., Prideaux, M., Rahman, S. et al. (2015). Localized drug delivery of selenium (Se) using nanoporous anodic aluminium oxide for bone implants. *Journal of Materials Chemistry B, 3(35),* 7090–7098. DOI 10.1039/C5TB00125K.

165. Kim, S., Ozalp, E. I., Darwish, M., Weldon, J. A. (2018). Electrically gated nanoporous membranes for smart molecular flow control. *Nanoscale, 10(44),* 20740–20747. DOI 10.1039/C8NR05906C.

166. Aw, M. S., Simovic, S., Dhiraj, K., Addai-Mensah, J., Losic, D. (2010). The loading and release property of nanoporous anodic alumina for delivery of drugs and drug carriers. *Proceedings of the IEEE,* 143–145. DOI 10.1109/ICONN.2010.6045213.

167. Thorat, S. B., Diaspro, A., Salerno, M. (2014). *In vitro* investigation of coupling-agent-free dental restorative composite based on nano-porous alumina fillers. *Journal of Dentistry, 42(3),* 279–286. DOI 10.1016/j.jdent.2013.12.001.

168. Fazli-Abukheyli, R., Rahimi, M. R., Ghaedi, M. (2019). Electrospinning coating of nanoporous anodic alumina for controlling the drug release: Drug release study and modeling. *Journal of Drug Delivery Science and Technology, 54,* 101247. DOI 10.1016/j.jddst.2019.101247.

169. Hong, C., Tang, T. T., Hung, C. Y., Pan, R. P., Fang, W. (2010). Liquid crystal alignment in nanoporous anodic aluminum oxide layer for LCD panel applications. *Nanotechnology, 21(28),* 285201. DOI 10.1088/0957-4484/21/28/285201.

170. Zhou, L., Tan, Y., Ji, D., Zhu, B., Zhang, P. et al. (2016). Self-assembly of highly efficient, broadband plasmonic absorbers for solar steam generation. *Science Advances, 2(4),* e1501227. DOI 10.1126/sciadv.1501227.

171. Davoodi, E., Zhianmanesh, M., Montazerian, H., Milani, A. S., Hoorfar, M. (2020). Nano-porous anodic alumina: fundamentals and applications in tissue engineering. *Journal of Materials Science: Materials in Medicine, 31(7),* 60. DOI 10.1007/s10856-020-06398-2.

172. Park, J. S., Moon, D., Kim, J. S., Lee, J. S. (2016). Cell adhesion and growth on the anodized aluminum oxide membrane. *Journal of Biomedical Nanotechnology, 12(3),* 575–580. DOI 10.1166/jbn.2016.2192.

173. Shi, Y. (2018). *Inhibiting the growth of lithium dendrites by employing the anodic aluminum oxide membrane*. Boston.

174. Mohan Raj, R., Raj, V. (2018). Fabrication of superhydrophobic coatings for combating bacterial colonization on Al with relevance to marine and medical applications. *Journal of Coatings Technology and Research, 15(1),* 51–64. DOI 10.1007/s11998-017-9945-2.

175. Lee, D., Go, M., Son, S., Kim, M., Badloe, T. et al. (2021). Sub-ambient daytime radiative cooling by silica-coated porous anodic aluminum oxide. *Nano Energy, 79(7528),* 105426. DOI 10.1016/j.nanoen.2020.105426.

176. Wang, S., Tian, Y., Wang, C., Hang, C., Zhang, H. et al. (2019). One-step fabrication of copper nanopillar array-filled AAO films by pulse electrodeposition for anisotropic thermal conductive interconnectors. *ACS Omega, 4(4),* 6092–6096. DOI 10.1021/acsomega.8b03533.

177. Fu, L., Wang, Y., Jiang, J., Lu, B., Zhai, J. (2021). Sandwich ion pool-structured power gating for salinity gradient generation devices. *ACS Applied Materials & Interfaces, 13(29),* 35197–35206. DOI 10.1021/acsami.1c10183.

178. Li, H., Wu, L., Zhang, H., Dai, W., Hao, J. et al. (2020). Self-assembly of carbon black/AAO templates on nanoporous Si for broadband infrared absorption. *ACS Applied Materials & Interfaces, 12(3),* 4081–4087. DOI 10.1021/acsami.9b19107.

179. Li, J., Wei, H., Zhao, K., Wang, M., Chen, D. et al. (2020). Effect of anodizing temperature and organic acid addition on the structure and corrosion resistance of anodic aluminum oxide films. *Thin Solid Films, 713,* 138359. DOI 10.1016/j.tsf.2020.138359.

180. Bunge, F., van den Driesche, S., Vellekoop, M. J. (2018). PDMS-free microfluidic cell culture with integrated gas supply through a porous membrane of anodized aluminum oxide. *Biomedical Microdevices, 20(4),* 98. DOI 10.1007/s10544-018-0343-z.

181. Ingham, C. J., Ter Maat, J., de Vos, W. M. (2012). Where bio meets nano: The many uses for nanoporous aluminum oxide in biotechnology. *Biotechnology Advances, 30(5),* 1089–1099. DOI 10.1016/j.biotechadv.2011.08.005.

182. Baskar, S., Vijayan, V., Saravanan, S., Balan, A. V., Antony, A. G. (2018). Effect of Al_2O_3, aluminium alloy and fly ash for making engine component. *International Journal of Mechanical Engineering and Technology, 9(12),* 91–96.

183. Zhu, J., Chen, C., Lu, Y., Zang, J., Jiang, M. et al. (2016). Highly porous polyacrylonitrile/graphene oxide membrane separator exhibiting excellent anti-self-discharge feature for high-performance lithium-sulfur batteries. *Carbon, 101(23),* 272–280. DOI 10.1016/j.carbon.2016.02.007.

184. Lee, Y., Kim, H. J., Kim, D. K. (2020). Power generation from concentration gradient by reverse electrodialysis in anisotropic nanoporous anodic aluminum oxide membranes. *Energies, 13(4),* 904. DOI 10.3390/en13040904.

185. Zarei, H., Saramad, S. (2018). The radiation gas detectors with novel nanoporous converter for medical imaging applications. *Journal of Instrumentation, 13(2),* C02053. DOI 10.1088/1748-0221/13/02/C02053.

186. Sarno, M., Tamburrano, A., Arurault, L., Fontorbes, S., Pantani, R. et al. (2013). Electrical conductivity of carbon nanotubes grown inside a mesoporous anodic aluminium oxide membrane. *Carbon, 55(2),* 10–22. DOI 10.1016/j.carbon.2012.10.063.

187. Gloukhovski, R., Freger, V., Tsur, Y. (2016). A novel composite nafion/anodized aluminium oxide proton exchange membrane. *Fuel Cells, 16(4),* 434–443. DOI 10.1002/fuce.201500166.

188. Hashimoto, H., Kojima, S., Sasaki, T., Asoh, H. (2018). α-Alumina membrane having a hierarchical structure of straight macropores and mesopores inside the pore wall. *Journal of the European Ceramic Society, 38(4),* 1836–1840. DOI 10.1016/j.jeurceramsoc.2017.11.032.

189. Chen, W., Wang, X., He, G., Li, T., Gong, X. et al. (2018). Anion exchange membrane with well-ordered arrays of ionic channels based on a porous anodic aluminium oxide template. *Journal of Applied Electrochemistry, 48(10),* 1151–1161. DOI 10.1007/s10800-018-1214-2.

190. Pervez, M. F., Mia, M. N. H., Hossain, S., Saha, S. M. K., Ali, M. H. et al. (2018). Influence of total absorbed dose of gamma radiation on optical bandgap and structural properties of Mg-doped zinc oxide. *Optik, 162,* 140–150. DOI 10.1016/j.ijleo.2018.02.063.

191. Mia, M. N. H., Habiba, U., Pervez, M. F., Kabir, H., Nur, S. et al. (2020). Investigation of aluminum doping on structural and optical characteristics of sol-gel assisted spin-coated nano-structured zinc oxide thin films. *Applied Physics A, 126(3),* 162. DOI 10.1007/s00339-020-3332-z.

192. Mia, M. N. H., Pervez, M. F., Hossain, M. K., Reefaz Rahman, M., Uddin, M. J. et al. (2017). Influence of Mg content on tailoring optical bandgap of Mg-doped ZnO thin film prepared by sol-gel method. *Results in Physics, 7,* 2683–2691. DOI 10.1016/j.rinp.2017.07.047.